INVESTIGATION OF FACTORS AFFECTING THE SILICONE RUBBER INSULATOR AND NANO-DIELECTRIC STRENGTH IN HIGH VOLTAGE POWER TRANSMISSION SYSTEM

A Dissertation submitted in fulfilment of the requirements for the Degree of

MASTER OF ENGINEERING
in
POWER SYSTEMS

Submitted by

Vinit Srivastava
801742024

Under the Guidance of

Dr. Bharat Singh Rajpurohit
Associate Professor
SCEE, IIT Mandi, Himachal Pradesh

Ms. Manbir Kaur
Associate Professor
EIED, TIET, Patiala

THAPAR INSTITUTE
OF ENGINEERING & TECHNOLOGY
(Deemed to be University)

2019

Electrical and Instrumentation Engineering Department
Thapar Institute of Engineering & Technology, Patiala
(Declared as Deemed-to-be-University u/s 3 of the UGC Act., 1956)
Post Box No. 32, Patiala – 147004
Punjab (India)

DEDICATED

To

My Mother & Nature

Investigation of Factors Affecting the Silicone Rubber Insulator and Nano-Dielectric Strength in High Voltage Power Transmission System

Vinit Srivastava
801742024

July 26, 2019

Declaration

Certified that the dissertation entitled, **"Investigation of Factors Affecting the Silicone Rubber Insulator and Nano-Dielectric Strength in High Voltage Power Transmission System"**, carried out at **Indian Institute of Technology Mandi, Himachal Pradesh** which is being submitted by Vinit Srivastava in fulfillment of the requirements for the award of **the M.E. in Power System**, to **Thapar Institute of Engineering and Technology, Patiala**, is a bonafide record of the candidate's own work carried out by him under guidance of **Dr. Bharat Singh Rajpurohit, Associate Professor, School of Computing and Electrical Engineering, Indian Institute of Technology Mandi** and **Manbir Kaur, Associate Professor, Electrical and Instrumentation Engineering Department, Thapar Institute of Engineering and Technology, Patiala.** The matter contained in this dissertation has not been submitted, neither in part nor in full to any other university or institute for the award of any degree.

Vinit

Vinit Srivastava (801742024)

Bharat

Institute Guide at IIT Mandi
Dr. Bharat Singh Rajpurohit
Associate Professor
SCEE, IIT Mandi

Manbir Kaur

Institute Guide at TIET Patiala
Manbir Kaur
Associate Professor
EIED, TIET, Patiala

ACKNOWLEDGEMENT

This dissertation has seen contributions from various individuals. It has been an honour to work under the supervision of Dr. Bharat Singh Rajpurohit, School of Computing and Electrical Engineering, Indian Institute of Technology Mandi, Himachal Pradesh. I am extremely grateful to him for his academic and moral support. I would like to thank him for encouraging the research and allowing me to grow as a researcher.

I would also extend my gratitude towards my supervisor Ms. Manbir Kaur, Associate Professor, Electrical and Instrumentation Engineering Department, Thapar Institute of Engineering & Technology, Patiala for her all guidance, academic and financial support from the institute. You provided me with the right direction and valuable comments for successful completion of my dissertation

This dissertation could not have been written without the continuous love and care from my fellow labmates, Adil Usman (PhD Research Scholar), Rajesh Pindoriya (PhD Research Scholar), Siddhant Kumar (M.S Research Scholar), SCEE, IIT Mandi. I owe them a lot. I am grateful to all faculty and staff of Indian Institute of Technology Mandi for their every bit of support.

I am indebted to Dr. R.S. Kaler, Head, EIED and Dr. S.S. Bhatia, DoAA, who have extended me all support to carry out dissertation work at IIT Mandi. I hereby acknowledge the support extended to me by TIET.

I have no word to thank my friends like Harish Sen, Rohit Garg and Pushpendra Kumar for their wholehearted affection, continuous admiration, and encouragement during all hard times.

Lastly, I feel grateful to my mother, my family, my teachers and Lord Almighty, who has showered his grace upon me during this period.

Vinit Srivastava

801742024

TABLE OF CONTENTS

LIST OF TABLES

LIST OF FIGURES

LIST OF ACRONYM

FEM:	Finite Element Method
SIR:	Silicone Rubber
COMSOL:	Communication Solutions
UV:	Ultra Violet
PD:	Partial Discharge
LDPE:	Low density polythene
XLPE:	Cross-linked Polythene
PDE:	Partial Differential Equations
TPJ:	Triple Point Junction
HV:	High Voltage
E-norm:	Normalized Electric Field
P-norm:	Normalized Polarization Density
FEMLAB:	Finite Element Method Laboratory
MATLAB:	Matrix Laboratory
NSDD:	Non Soluble Dust Density
SiO_2 :	Silicon Dioxide
$CaCO_3$:	Calcium Carbonate
$SrTiO_3$:	Strontium Titanate
Al_2O_2 :	Aluminum Dioxide
Ta_2O_5 :	Tantalum Pentoxide
$BaTiO_3$:	Barium Titanate
TiO_2:	Titanium dioxide

ABSTRACT

In case of overhead transmission line insulator, five cases have been investigated from the electric field and polarization density distribution point of view. All cases focus at triple point junction of the water drop by comparing dry air to humid, by increasing the volume, by increasing the contact angle, by increasing the permittivity of pollution layer and by the presence of pollution particle. This study shows the simulation of the water drop at the 90-degree contact angle on clean silicon rubber insulator under high voltage stress in 2D space dimension is shown, by using the finite element method based software. The simulation results provide deep insights about relation on local electric field intensification with environmental changing parameters.

Where in case of nano composite, as the permittivity of the nanocomposite increases, comparison to ellipsoid water void, by increasing the permittivity of the base material and nano filler enhances the nano dielectric strength and by decreasing interparticle distance. Nano interface is considered as the cause for better insulation strength, but as its understanding is largely unknown. The simulation results show many aspects to enhance the dielectric strength from exploring interface. At last, a new approach to configure two particles has been investigated which results in finding the best configuration for better insulation.

Finally, the practical importance of this work is that it can be used to understand nano interface in nanodielectrics and future investigators can use it as a guide to choose material for their next experiment in order to obtain better insulation.

CHAPTER 1
INTRODUCTION

1.1 Introduction

It is a known fact that, when power is generated, it has to be transmitted. Transmission of energy can be done by two means first by overhead lines and second by underground cables. In transmission, reliability demands the transfer of electrical energy should be safe and continuous from any kind of leakage, flashover and short circuit to occur in the power transmission system. Hence the element which is responsible for addressing this issue of leakage and flashover is called an insulator.

Motivation behind choosing this dissertation area, originated at Indian Institute Technology Mandi, Himachal Pradesh. During my stay, I saw something fascinating at the mountain in front of electrical machines lab. It's a cloudy day and I saw transmission towers situated at the hills, fading in and out between clouds, as shown in figure 1.1. So, Inspiration driven by the electrical physical phenomenon of nature, I decided to investigate the dynamic-electrostatic phenomenon occurring at the water drops on the high voltage polymer insulator. The motivation behind this dissertation is to understand the electro-hydrodynamic behaviour of water drops on silicon rubber insulator under the influence of high voltage transmission lines, lies in heart of nature. The motivation behind insulation study has also turned into investigating the insulation material of underground cable.

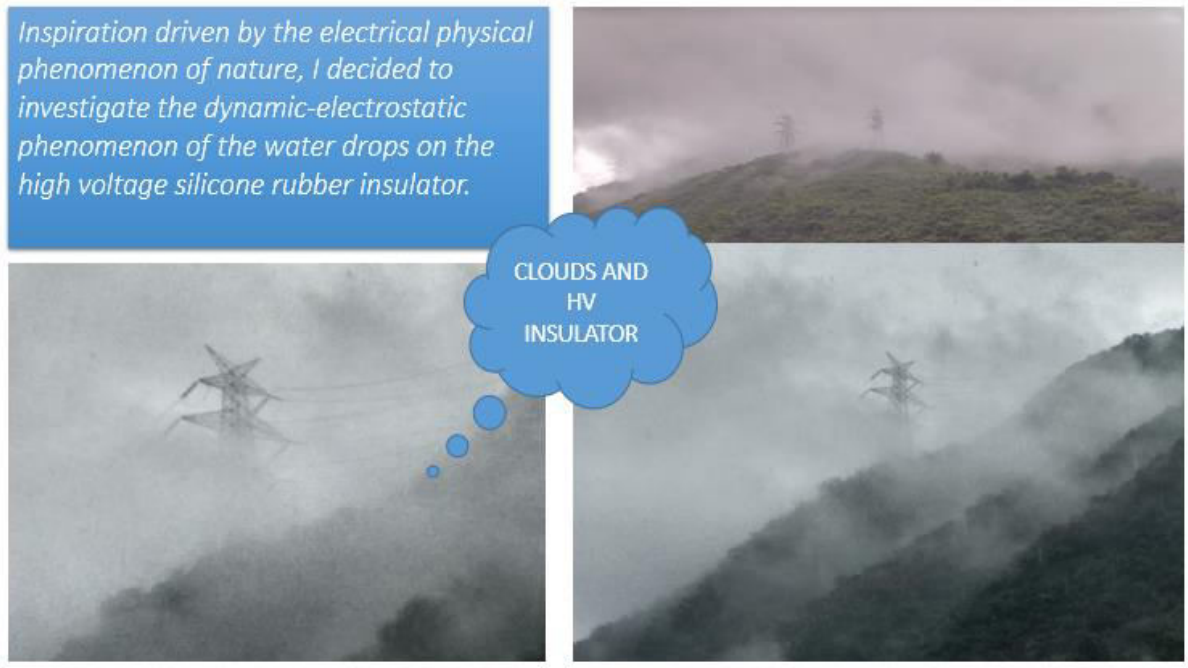

Figure 1.1: The atmospheric scene in front of the special electrical machines lab at I.I.T Mandi

1.1.1 Overview of Overhead Transmission

Role of high voltage transmission lines in today's world has been increasing rapidly with the increasing power demand. A transmission line consists of ground wires, insulators, line conductors as shown in figure 1.2. The purpose of the insulator is to provide mechanical support as well as insulation strength to the overhead line. Insulation is the vulnerable part on transmission lines, as it the only element which carries the reliability factor of electrical energy transfer from one point to another. Most of the time, overhead line insulators are exposed to harsh environment like dust, fog, wind, pollution, snow, humidity, ultraviolet and lot of heating etc. Those are responsible for the change in the properties of materials and affects the life of insulation. It is utmost necessary to investigate the electric field stress patterns on insulators under different environmental conditions to ultimately ensure the reliability requirements of the power system. Types of insulation material are available e.g. glass and porcelain, which are being used in traditional days [1]. Though they have issues in aspects like weight, ease to break and pollution problems. Continues contamination leads hydrophobicity of the material to hydrophilicity [2], for the solution now a day we have polymer insulators. Detailed study of polymer insulators, environmental exposures and their harmful effects on degradation of insulation strength has been rigorously surveyed in upcoming literature survey.

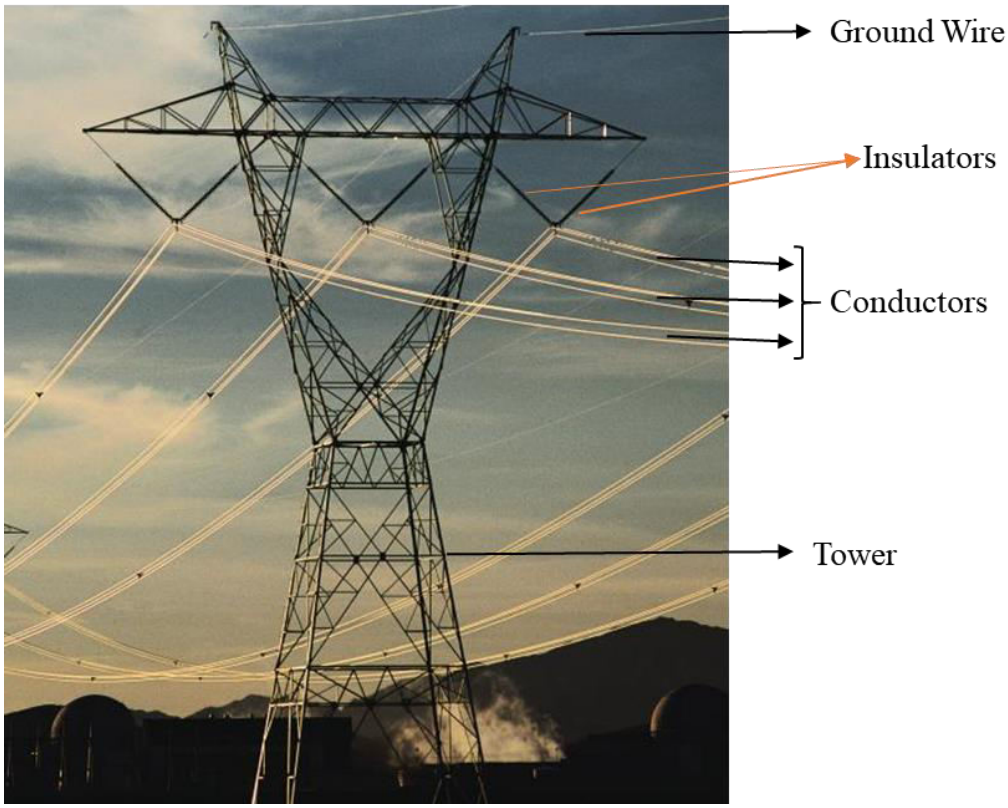

Figure 1.2: High Voltage Overhead Transmission Line

1.1.2 Overview of Underground Cables

As the world is moving towards renewable energy demand, penetration of renewable modes of electrical energy transmission increased to manifolds. Hence, for modern generation the energy transmission with underground high voltage direct current/alternating current cable technology is natural outcome. The key difference in overhead and underground transmission line is in the requirements of insulation. Overhead transmission line does not need any additional layer of insulation, as air (Maximum breakdown strength of 30kV/cm) is there around the conductor and spacing between the bare conductors is adjusted to avoid any flashover under normal operating conditions. On the other hand, underground transmission line, the conductors are wrapped in insulation layers and are placed in close proximity. The thickness of the insulation is adjusted according to operating voltage level of cable.Insulation layer is the most fundamental thing in cable material's technology as shown in Figure 1.3, which presents the schematic diagram of the high voltage cable. In market there are four categories of cable based on the type of dielectric material namely; dissertation based, oil filled, polypropylene dissertation laminated and polymer based cross-linked polyethylene (XLPE). Though, these days XLPE has the maximum share in the market and research because of its principal advantages like light weight, higher operating temperature, chemical stability etc. [3]-[5]. Semiconducting layers (b and d in figure 1.3), made up of carbon black, are placed to allow the homogeneous distribution of electric field for preventing partial discharge and provide smooth contact between conductor and insulator. The metallic screen layer helps to uniform the field distribution with grounded condition. The outer most layer, which is the protection jacket for the cable.

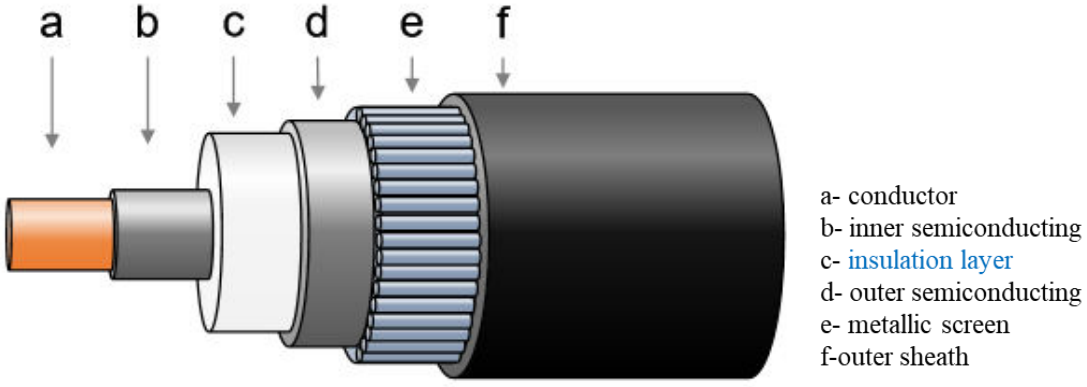

Figure 1.3: Schematic diagram of a typical cable

These days, most of the research work is dedicated to the improvement of the material technology of cable insulation. The polythene material has been used mostly is the cross-linked polythene (XLPE) but, with the advancement in nano-technology resulting the

advanced nano-composite insulation or nano-dielectric material. Figure 1.4 shows the different applications of nanodielectrics like in partial discharge resistance, space charge suppression, high energy storage, high thermal conductivity etc. Nanocomposite material means filling nano-particles in the base XLPE material, which results in high breakdown strength, additionally with other benefits like improved mechanical strength, durability and thermal strength. Varieties of nano filler particle are available which are mixed with base materials with standard mixing procedure. Nano-composite material shows unique potential properties which is majorly guided by the nano interface area in that material. The largest fraction in a nano-composite is nano-interface area. The mystical area whose physics is still unknown on large extent.

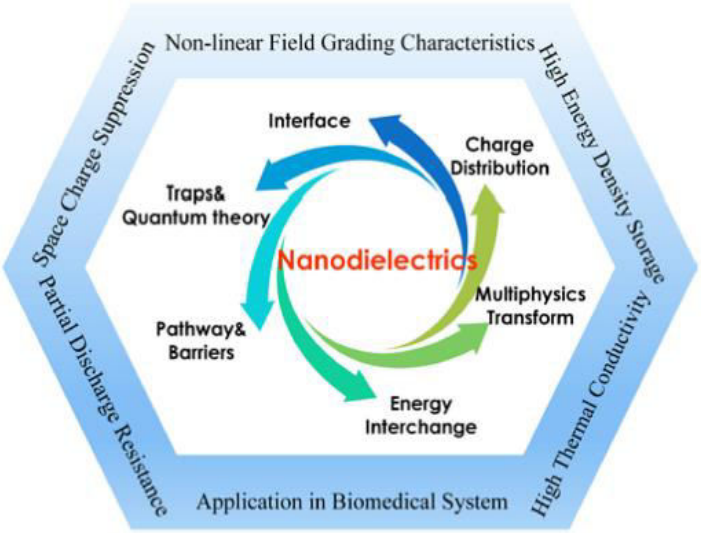

Figure 1.4: Features of Nano-dielectrics

This dissertation focuses on the judgement of choice of materials with intentions to see the improvement in the nano-composite insulation, detailed study of cable insulator, has been surveyed in upcoming literature.

1.1.3 Overview on Software Tool.

Figure 1.5 presents three numerical methods and their limitations those are preferred to carry out anlysis. First is finite difference method which simplifies the nonlinear problem to linear one, hence making computation easy and fast however, is limited by the characteristic values calculations at the curved spaces.

Second the boundary element method is a numerical computational *method* of solving linear partial differential equations, which have been formulated as integral equations applicable to linear and open domain problems, but is limited by not being able to solve nonlinear problems.

Finite element method (*FEM*) is a numerical technique based on the principle of discretisation and is used to perform *finite element analysis* of any given physical phenomenon. Literature study about numerical methods suggest that finite element method is the most used and most robust method for solving numerical problems.

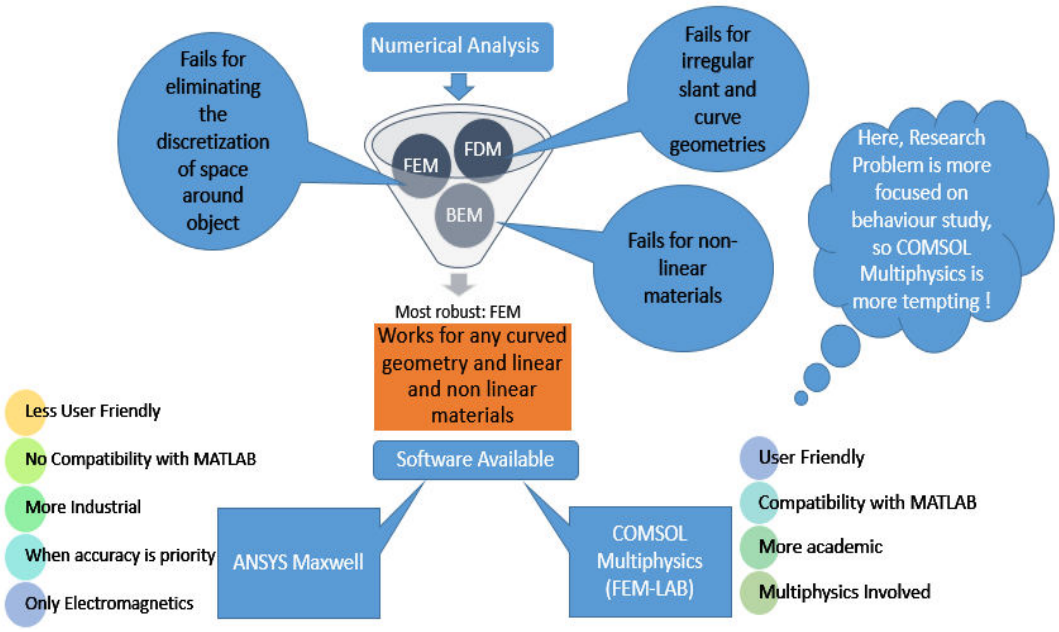

Figure 1.5: Numerical methods and software tool available

To carry out finite element analysis to investigated the behaviour of physical phenomenon in electrical engineering applications, ANSYS Maxwell and COMSOL (Communication Solutions) Multiphysics are the most preferred tools. Here, figure 1.6 gives the overall expression of the work, which has been systematically carried out in this dissertation work.

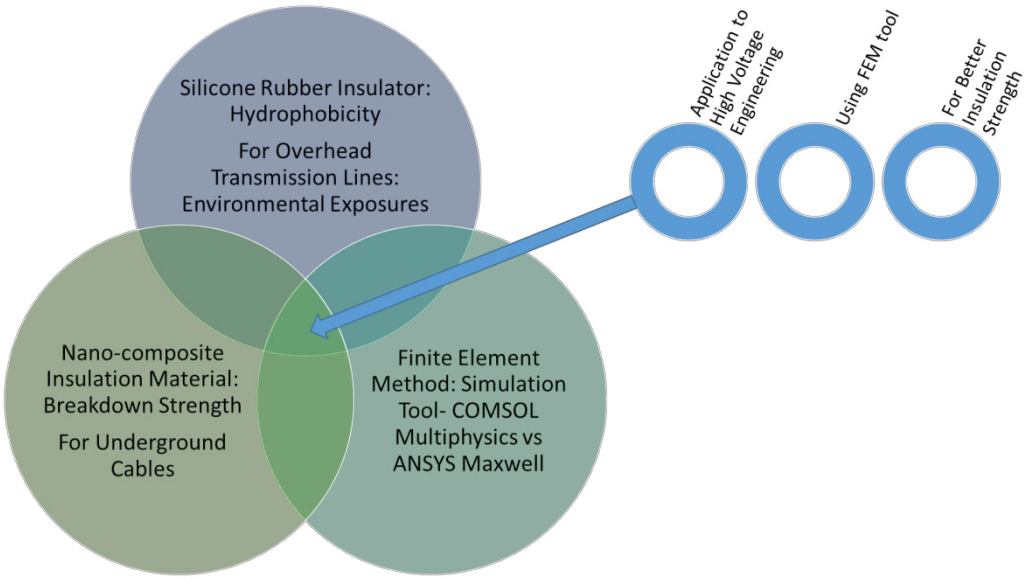

Figure 1.6: Overall expansion of dissertation work

1.2 Literature Review

1.2.1 Polymer Insulators: The State of Art

When electric power is generated, it has to be transmitted over a large distance from generator stations to load centres. When it comes to transmission there are two ways to transmit the energy, one from overhead transmission lines and other from an underground transmission line. The work has been done for both kinds of insulation element. First investigation of the factors which affect the high voltage overhead transmission lines during the presence of water drop under different environmental factors and the second investigation has been done with an intention to see the factors, which improve the nanodielectric strength of high voltage cables.

F. Aouabed et. al. (2018) considered the fact that, in today's world of the electric power utility, two things are widely accepted, first is transmission at high voltage and second is the polymer insulators. The role of the transmitting energy at high voltage is to flow the power to thousands of kilometre with minimum loss of electrical energy. Where the role of polymer insulators has the responsibility to carry the reliability factor in transporting the electrical energy. This insulator is an electrical equipment which supports the overhead lines and insulates the high voltage conductor from the pylon. Polymer insulator significantly drops the electrical conduction, induction, and potential effects from entering into the tower's pylon. Authors have experimentally and numerically investigated the water drop in presence of electric field only for changing conductivity, number of water drops and its position from the electrodes. All established investigation, found that the triple point junction is the most critical point where the local electric field caused by deformation, before flashover. This the real and first cause of all degrading phenomenon occur at SIR insulator [6]. From this dissertation the knowledge about electromagnetic Maxwell equation (Gauss Law) can be used in the FEM software to calculate the electric field is known. Other things like data of dielectric constant of SIR, water drop has been taken as 3.9 and 81 respectively, which can be used in this research work.

Reynders et. al. (1999), N. Yoshimura et. al. (1999) and C. Zhao et. al. (2015) concluded that the use of polymer insulator in distribution as well as in transmission is increasing at high rate. It has been rapidly increasing because of the multiple advantages like it's lightweight, high mechanical strength and its property of having high hydrophobicity. Low surface energy is one of the most demanding properties in insulators where the SIR insulator is dominating over all others insulators in the power system. The SIR has become the first choice by the high voltage power apparatus utilities. The hydrophobicity of SIR has widely accepted in today's world of the insulator. However, the material got degraded after long exposure to

the environmental conditions such as acid rain, UV rays and salt fog. Many investigations under contamination conditions point towards that fact that, the flashover and dry band arc formations are the major reasons for the poor performance like the ageing of the polymer insulator [7]-[9]. This dissertation provides the reason to investigate environmental factor which produces dry band arc, ageing and the degradation of hydrophobicity of SIR to become hydrophilic.

R. Hackam et.al. (1998) and E.A. Cherney et. al (1996) has noted that in the last two decades, the polymeric material has emerged as the most practised outdoor insulator. This type of insulators in the outdoor application is increasing, because of its high efficiency and improved characteristics. Having better contamination performance, especially because of its hydrophobic surface. SIR insulator is widely accepted insulator as it has low surface energy and property of recovering hydrophobicity. However, the material loss its hydrophobicity during severe conditions and surface become hydrophilic[10]-[11]. From this established investigations, it is clear that the area of interest is the triple point junction or critical area (interface of water, air and insulator). The triple point is the point where local electric field intensification occurs under applied electric fields in every circumstance. Hence it is important to see the effect on triple point junction under changing thin layer pollution permittivity, as one of the objectives to this research work.

Zhicheng Guan et. al. (2005) investigated water drop in presence of electric field for corona discharge because of local electric field intensification at the triple point junction, establishing the relationship between inception voltage and different arrangement in the water drop. The inception voltage had investigated by changing contact angle, volume and multiple drops. Experimental model used here is based on the knowledge, that there are two kinds of location for the drop, one is pedant on the insulator shed which is facing horizontal electric field and the second is clinging drops on the core which is mostly under vertical electrical field region [12]. Experimental results showed that as the number of drops, contact angle and volume increases that inception voltage reducers. The understanding of the reason to use the particular geometry by the Zhicheng Guan *et. al.* has been taken in this research work for the reason to investigate the water drop pedant on the insulator shed which is facing the horizontal electric field. Here the experimental investigation for the drop pedant over the insulator shed, as shown below in Figure 1.7. This geometry consist of 100 mm long cylindrical electrode, where the insulator slab is 50 mm × 50 mm in height and width. Water drops are setting in pedant fashion, subjected to horizontal electric field . For the same reason, this dissertation work uses the same arrangement for all water drop model of investigation.

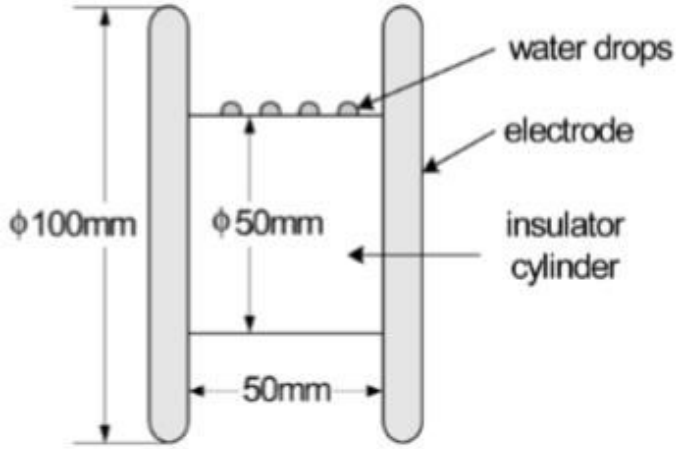

Figure 1.7: Model used in the experiment [12]

Mr. G. Satheesh et. al. (2012) worked on understanding the nature of dust layer thickness of the water drop electrostatic behaviour, first, the numerical calculation has been done with and without dust layer. After that, the thickness was increased with 0.5mm to 1.5mm of thickness for cement and plywood dust. Results showed that as the thickness of dust layer increases the electric field has decreased, where the potential distribution did not affect much. From this, authors are trying to confirm the electrical performance of SIR is better over other insulators [13].

S. Feier-Iova et.al (2009) proposed that the water drop under electric stress, the electric field distribution has been completely based on permittivity of the material taken as capacitive distribution. The deformed droplet i.e. the formed Taylor cone started to eject the streamers of very small electrically charges droplets from the Taylor cone (triple point junction) an important relationship between PD inception electric field strength and atmospheric conditions like humidity. Breakdown field strength is dependent on humidity factor: it decreases with increasing absolute humidity [14]. Authors has shown the serious concern for the triple point junction in relation to humidity increase. There is little knowledge about this triple point junction during its very initial conditions when no deformation has been taken place and how the TPJ nature affected in result to changing polarization density and electric field. It's true that the deformation of the water drop is the real cause of all partial discharge activities, but what happens to this cone area when no deformation, the discharge has taken. The investigation in the change in polarization density when a water drop is at perfectly semi sphere geometry of contact angle of 90°, give rise to the one more objective which has been done in this research work

Wang, X et.al (1999) and Wang, Song et. al. (2013) both noted that the power generation stations in most of the countries are situated far away from the load centres. The electrical

energy has been transferred under various environmentally polluted situations like ultraviolet, wet or humid environments, desert areas, industrial emissions etc. Polymer insulators close to coastal area face micrometre size sea salt particles whereas those in the cities exposed to dust, ash and many other kinds of fine dust airborne particles which slowly and continuously accumulate over the insulator surface and form a dry arc or conductive paths over the surface of the insulator [15]. The surface roughness, pollution particles and lack of hydrophobicity of SIR are interrelated as clearly shown by Wang, Song et. al [16]. The presence of these grain size micrometre particle in any form made a virgin homogenous surface to become heterogeneous by settling over it. The chosen surface roughness of these particles with the average grain size range from 50 μm to 300 μm [15]-[16]. This research laid the foundation for the need to study the effect of the presence of non-soluble particles or settled surface micrometre bumps on SIR surface and how they interact electrostatically with the water drops on insulator surface.

According to **IEC standard 2008** [17], the two major causes of pollution, which leads to flashover are solid pollution (Type A) and liquid pollution (Type B). Solid pollution with non-soluble deposited over the insulator form the conductive path when moisture is present over it in the form of tiny drops, leakage current start to flows over it. The characterization of pollution particle by the term NSDD as non-soluble deposit density started to build a layer of it associated with the island, desert, fog, mist, dew pollution types. Therefore, it is required to understand the behaviour at a triple point junction in the presence of roughness of the surface, i.e. the presence of pollution particle which is non-soluble and deposited over the surface due to continuous exposure of it. Hence, in this research, the systematic investigation of the presence of a particle effect on the water drop's TPJ has been done. The four case needed to be studied which shows how the electric field and polarization density at TPJ of water drop change under the presence of a particle. As particle comes near to water drop (Case I), as relative permittivity of the particle is increasing (Case II), the number of particles is increasing (Case III) and as particle size is decreasing (Case IV). In every case of this investigation, the effect we are going to see is by increasing or decreasing very minimally because to make the model close to the initial level of investigation for understanding the nature of it.

G. Moustafa et. al. (2016) conducted the experiment in concern to develop a long transmission lines enrouting through desert areas. Study about the breakdown performance of the air gaps at different sand concentration, sand speed and size has been carried out with the conclusion that as the sand size is decreased, the number of sand particles increase, the number of sand deposited over electrode led to decrease in the breakdown voltage [18].

In general, there is lack of investigation to visualize and analyse the change in the potential distribution, normalized electric field and polarization density when a water drop is placed on the insulator surface with an initial shape (hemisphere) and contact angle (90°) corresponds to the hydrophobicity of wetting class (WC)-1 under humid air conditions and then it is compared with dry air boundary conditions. In this research work, one more objective is to investigate the water drop under high voltage electric stress with very initial stages, assuming the water drop on the perfectly clean hydrophobic surface. As it is known from the established research till now, is that, every initial partial discharge activity is the result of an initial electrostatic and electro-hydrodynamic phenomenon occurring under every initial boundary condition. Breakdown field strength is dependent on humidity factor: it decreases with increasing absolute humidity. Hence it is important to know the initial stage development occurring with water drop when the distribution is governed by the permittivity of the material, characteristics of humid air boundary conditions and its effects on electrostatic parameters. Other changing parameters will be implemented by changing the volume of the water drop again to know the initial changes happen with polarization density by changing the volume of water drop again without the deformation of the water drop, which has been done as one more objective of this research work.

This work analysis is based on numerical calculations of Maxwell Equation for seeing the potential, electric field and polarization density distribution. All electrostatic parameter calculations were numerically computed using the Finite Element Method (FEM) tool. The simulation has been performed under electrostatic physics in AC/DC module with the 2D model. The foundation of designing the SIR insulator depends on our microscopic knowledge of enhancement of the local electric field and polarization density of drop. Hence, in summary, this work contribution can be used to learn effectively about the behaviour of the water drop on SIR insulator surface. In this research work, as most of the concern is on “How the electrostatic nature of the triple point junction has influenced under different circumstances”. Here, because to understand the nature of this particular physics “COMSOL Multiphysics” is sufficient rather than accuracy, expectations of use of MATLAB and the availability of COMSOL Multiphysics has been used in this work.

1.2.2 Nano Dielectrics: The State of Art

Andritsch, T.M. (2010) noted that nanotechnology fundamental aspect is its size, it is evident from the Figure 1.8, is that, as the size of the nanoparticle decreases the interface area become more important. Nano-particle properties become unexpected as the interface area came into existence. Nanotechnology in power engineering has been increased to manifolds, especially

in the application with nano-fluids in power transformers, layered nano-filler in the solar cell. Initial work and findings in this nano interface area seem magical, there are many questions on the behaviour and nature of the nano interface is still unanswered. Numerous authors are working to in nano-composites, to decrease the partial discharge activity and other treeing effects, and they are successful. But the reason and nature of this still a lack of understanding. The purpose of this research works to go deeper at the level of the nano - interface area by using the finite element simulation software [19].

S. Zhong *et.al* (2018) reviewed nano-dielectrics and concluded that as the size of the nanoparticle decreases, the volume fraction of the interface area in the composite increases which could result in many benefits like space charge suppression [20], high energy density storage [21]-[22], reduced partial discharge (PD) activity [23] etc. The interface area is complicated in its physics and it cannot be understood clearly by single theoretical model. Nano-dielectrics are used at a high rate in electronic circuit into high voltage applications in [24]. The Classical theoretical model proposed by Lewis's diffusion electrical double layer model in [25] and Tanaka multicore model in [26] have already been established.

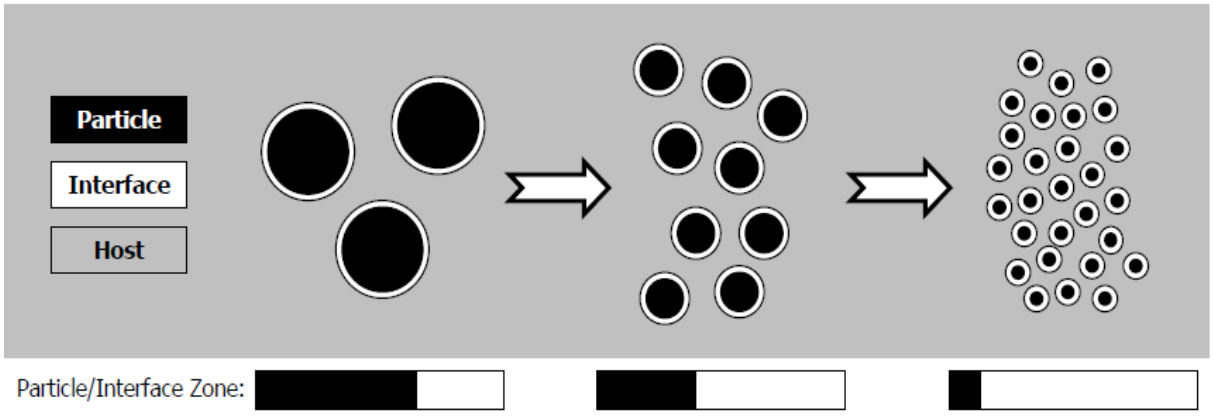

Figure 1.8: Illustrating the effect of the size of nanoparticle on interface area

Barber P. *et.al.* (2009) reviewed about the polymer composites and nano-composite dielectric material for pulsed power energy storage suggested that, there is strong interaction between the polymer and filler particle. Interface polarization is responsible for the enhanced dielectric performance, because of its high molecular polarizability. The extensive review of this dissertation concludes there is little knowledge on how the interface changes the electric breakdown strength. The data of different dielectric permittivity material used to investigate the nanocomposites research work to model effective permittivity of the nano filler [27] is given in Table 1.1.

Table 1.1: Dielectric Constant of the Nano Fillers

Nano-filler	Dielectric Permittivity
Silicon Oxide SiO_2	3.9
Calcium Carbonate $CaCO_3$	4.5
Aluminum Oxide Al_2O_3	9
Tantalum Pentoxide Ta_2O_5	22
Titanium Oxide TiO_2	80
Barium Titanate $BaTiO_3$	170
Strontium Titanate $SrTiO_3$	2000

Peng Simin *et. al.* (2016) proposed that local dielectric property of the interface area eventually decreases below the dielectric constant of low-density polyethene (LDPE). The TiO_2 as a nanofiller investigated experimentally on LDPE, experimental microscopic mechanism of dielectric effect of interface the mobility of chain segments is bound and interfacial polarization go influenced in such a way that the permittivity of interface got decreased, which they called as the dielectric effect of the interface. FEM simulation run has been carried out for the permittivity values of 80 as nano-filler, 2.25 for LDPE and local dielectric constant of the interface was found to be 1.5. This experiment has shown the method to investigate the local dielectric property of nano-composite which inspires to investigate further to study the interface [28].

D. Kavitha *et. al*. (2017) have studied the effect of filler parameters on the electrical properties of nano-composites. The concept of interparticle distance estimation has been considered and discussed how the particle size, shape characterize the nanoparticle interface area. It has been observed the filler concentration increases the region of enhanced electric field which in turn reduces the breakdown strength. This reducing trend has been observed as the filler interparticle distance becomes equal to particle diameter. The experimental work here performed is by considering the epoxy base material with fore types of filler, named as TiO_2, Al_2O_3, $CaCO_3$ at different concentrations, in every case, the effective relative permittivity has increased with the presence of higher permittivity material in the nanocomposite [29].

Wenxuan Wang *et. al.* (2017) proposed the micro and nanoparticle composites at a different level of concentration, that produced the blocking effect to tree from its propagation. The experiment showed that the interface area of the nanocomposite has been much more than microparticle, overall the time taken to propagate is more so the breakdown time increase much in the micro-nano composites. It has been concluded that as the interface polarization increases the inhibition of charge injection and movement reduces the chances to break the molecular chain and causes a large number of traps and voids to be restricted in the interface area which overall increases the average trap depth which further increases the resistance to electrical tree propagation. Hence this research provides a new way to increase the reliability and durability component of the material [30].

Xin Zhang *et. al.* (2014) proposed and demonstrated the induction of hierarchical interface with high relative permittivity on the nanocomposite by preparing TiO_2 embedded with $BaTiO_3$ via the process of facile electrospinning, symbolise as TO@BTO. Significant effort has been imposed to induce higher interfacial polarization hence to achieve the higher relative permittivity of the whole composite [31]. Authors proposed and demonstrated that the hierarchical interface induces high relative permittivity on the nanocomposite by preparing TiO_2 embedded with $BaTiO_3$ via the process of facile electrospinning, symbolize as TO@BTO by using this two material. By this way, the overall permittivity of the material has been increased from 29 to 41. Hence this dissertation gives two main objectives to understand the interface area in a new way, which are going to be implemented in this research work. First objective is by investigating this hierarchical configuration under four cases First by choosing the inner nanomaterial in decreasing order of their relative permittivity and increasing the outer nanofiller material (Case I), Second case by choosing the inner nanomaterial in increasing order of their relative permittivity and increasing the outer nanofiller material (Case II), Third case by choosing the inner nanomaterial in decreasing order of their relative permittivity and decreasing the outer nanofiller material (Case III), Forth case by choosing the inner nanomaterial in increasing order of their relative permittivity and decreasing the outer nanofiller material (Case IV). The second objective is by increasing the relative permittivity of the overall sample without actually embedding the nanoparticle in the sample and seeing its effect on the air void, for instance, to confirm that nanocomposites give better insulation even in case of air is trapped in the sample.

The need of the time is to see the effect on the nano-dielectric interface, responsible for the electrical behaviour of breakdown strength for the nano-composite and preventing from any kind of possible partial discharge. **Andritsch, T.M**.[19] discussed the need to understand the nature of nano interface to understand the behaviour of nanocomposite to enhance or modify

the insulation material in the way as the application requires by using nanomaterial. In the review dissertation on nanodielectrics, **S. Zhong *et. al.*** [20] discussed the need to give special attention to the interface area, where the direct benefits come by decreasing the size of the nanoparticle. This brings the first reason to investigate its effects by increasing the thickness of interface area in the simulation model at the nano level, so to increase the knowledge about interface behaviour in the field of nano-interface at a theoretical level it's physics. **Barber, P *et. al.*** [21] reviewed and concluded that the interface polarization should be enhanced to increase the breakdown strength of the nanodielectrics, which give direction to the investigation for what kind of electrostatic polarization density nature is required for better insulation of the material. The experiment conducted by the **Peng Simin *et. al.*** [28] realized the new knowledge on the behaviour of interface guided by relative permittivity of the material, showed that the dielectric permittivity of the interface is lower than the base material. Believing on his experimental study about this unique behaviour of the interface, it has been decided in this research to investigate about how polarization density and electric field changes if the relative permittivity of the interface increases from below the value of the polymer base to above its value as one of the objectives of this work.

1.2.3 Finite Element Method: A Review

The field distribution around the SIR insulator surface with water drop will provide a better understanding during dust contamination and hydrophilicity of the surface under degradation. Moreover, the prediction of the dry band arc formations and ageing will become more accurate. Detecting the electric field and polarization density distribution in practice is a difficult and complex process by experimental methods. Investigating and calculating the electrical parameters to micro and nano level with help of experimental instruments is a very costly and difficult, but with the help of computer-based software, it is possible to calculate the parameters at such an extent to understand the nature. When understanding the nature of physical reality is the first most priority in science, these kinds of simulation software are found to very useful. Hence in this research work, the electrostatic parameters have been investigated at the very critical area called as triple point junction (TPJ) which is just existing in few micrometres to millimetre range. So, the numerical technique is used to obtain the electric field and polarization density calculations around water drop.

R. G. Olsen et. al. (2000) and E. Asenjo et. al. (1997) notifies that all calculations can be achieved by the well-established method called as Finite Element Method (FEM). The FEM was introduced in 1960 and till 1965 it comes into the application with electrical engineering problems. At present, the FEM is broadly used in electrical engineering, numerical calculation

methods for analytically quantifying and optimizing the insulator performance under all electromagnetic field analysis [32]-[33].

The finite element methods used to discretize the solution domain into a very small finite number of elements, every element node has its characteristic equation or the governing equations solved which has solved simultaneously and predicts the behaviour of the model. Solutions values are obtained by solving the discretized partial differential equations (PEDs) by using FEM.

FEM like software is very advantageous when following benefits are a major concern.

1. Optimization of product, performance and economy.
2. Reduces development time and testing requirements.
3. Safety improvement.
4. A higher degree of freedom in the analysis the physics by visualization.

In the market, there are many software available from free to paid licenced ones, but ANSYS Maxwell and COMSOL Multiphysics have dominated over all available software according to there various advantageous. In this research work, COMSOL Multiphysics has been used here in the dissetation work because of its availability at first and the following advantage over ANSYS Maxwell according to the nature of the problem in this research work.

In [34] *COMSOL Multiphysics* is oriented more towards the academia, a greater degree of freedom when the problem is existing more at the fundamental level of physics and accuracy is not a critical issue. It has many user-friendly and compatible with *MATLAB* software tool. *ANSYS Maxwell* is more Industry oriented tool, dedicated to core engineering problems where accuracy can't be ignored at any cost. It is robust and needs a lot of coding for different engineering problems with having a very strong mesh inside the software. One of its current disadvantages is an incompatibility with the *MATLAB* software tool.

1.3 Problem Statement.

Two types of insulator material which are being used in both overhead and underground transmission lines are SIR insulator, low-density polythene, high-density polyethene and epoxy material.

For overhead insulators, SIR is well known for its hydrophobicity in overhead transmission lines, because of its different environmental exposure like dust, pollution and water which leads to weak the insulation strength, causes flashover and ultimately converts the hydrophobicity of the SIR to hydrophilic in nature. Researchers have demonstrated the effect on triple point junction during increasing the number of drops, a position from the electrode, changing volume and after deformation of the drop. There is a lack of knowledge from three

perspectives, first investigation at the microscopic level, second at the very initial level of investigation when no deformation takes place and third is to investigate the drop's triple point junction from polarization density. Figure 1.9 shows the pictorial representation of the problem statement for overhead insulator.

It is unfavourable, complicated and difficult to investigate the effects of changing contact angle, volume, pollution layer, the presence of micrometre non-soluble solid pollution particle on triple point junction at such a microscopic level by numerical calculation of polarization density and electric field experimentally. So, as it is the behaviour study it is possible to investigate it in finite element software and results will be used by many researchers to get insights about the direction and to learn more effectively about the factors which cause loss of hydrophobicity.

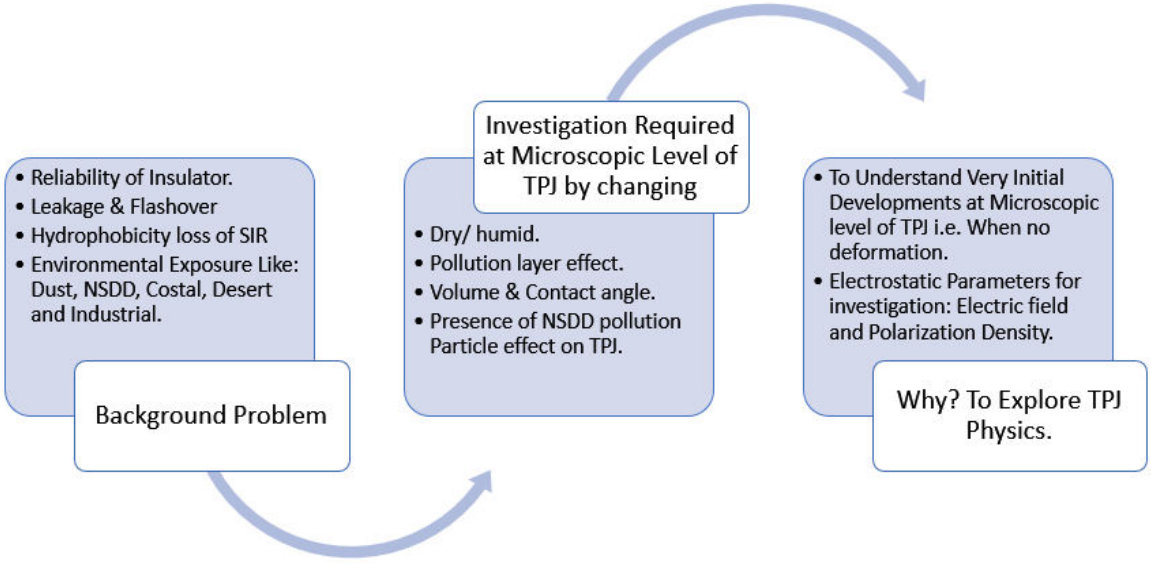

Figure 1.9: Pictorial representation of the problem statement for overhead insulator

For underground insulations, Figure 1.10 shows the pictorial representation of problem statement subjected to nanocomposites. They are well known for its enhanced breakdown strength and the physics of the nano interface is still unknown. So, in reference to acquiring the knowledge about interface by implementing different configuration by arranging two nanofiller in a concentric way, by changing the thickness of the interface, by changing nano filler, polymer base, interspace distance, by presence of water void of different shape in order to study the interface behaviour by using finite element method.

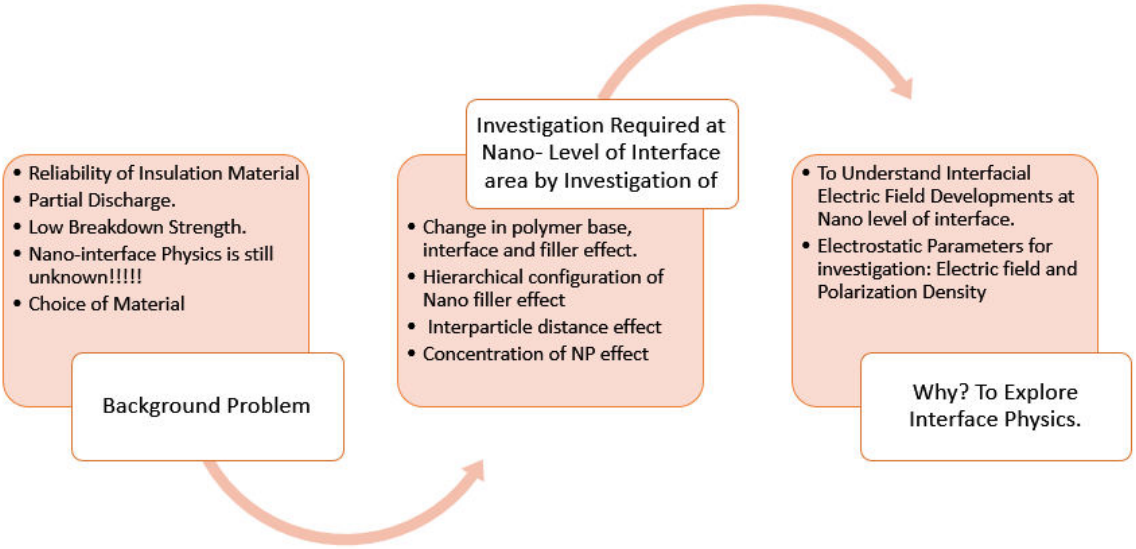

Figure 1.10: Pictorial representation of the problem statement for nanocomposites

1.4 Objectives

The objectives include the simulation models of water drop under various environmental conditions and model for understanding nano-dielectric strength by using FEM software:

Objective 1: To investigate the factors affecting the SIR insulator in the high voltage overhead power transmission system. The objective has been achieved by changing the factors like comparing dry to humid air conditions, changing pollution layer permittivity, volume, changing contact angle of the water drop and by investigation the presence of particle near the Water Drop

Objective 2: To investigate the factors enhancing the nano-dielectric strength in the high voltage overhead power transmission system. The objective has been achieved by changing sample permittivity and its effect on water void, by changing base material and nano filler.

The normalized electric field distribution and polarization density has been taken as reference parameters to analyse the behaviour in all cases of investigation in this dissertation.

1.5 Dissertation Outline

The study has been divided into four chapters, as follows.

- ✓ **Chapter 1:** includes introduction, literature review, purpose and objectives for the polymeric outdoor silicon rubber insulator and nano-dielectric materials.
- ✓ **Chapter 2:** includes numerical investigation by comparing dry to humid air conditions, changing pollution layer permittivity, changing volume, changing contact angle of water drop, pollution particle effect on water drop under high voltage SIR insulator.

- ✓ **Chapter 3:** includes numerical investigation by considering water void, different shapes of void, changing interface permittivity, changing base material and nano-filler, by changing interparticle distance and concentric configuration of two nano particles.
- ✓ **Chapter 4:** Conclusion and the Future Work are presented.

CHAPTER 2

OVERHEAD POLYMER INSULATOR UNDER HIGH VOLTAGE

2.1 Introduction

In this chapter, five cases have been investigated from the electric field and polarization density distribution point of view at water drops TPJ under HV stress.

- The first case of investigation is by comparing humid and dry air condition for the water drop on the clean SIR insulator surface under the influence of applied electric stress.
- The second case of investigation is by changing the volume of the hemispherical water drop on the insulator surface under the influence of applied electric stress.
- The third case of investigation is by changing the contact angle of water drop on the clean SIR insulator surface under the influence of applied electric stress.
- The forth case of investigation is by changing the dielectric constant of the dust layer contamination under the hemispherical water drop of the insulator surface under the influence of applied electric stress.
- In fifth case, there are fore subcases which have been investigated by considering the particle presences in presence of water drop. In all four subcases, the water drop is taken at a 90° contact angle on the SIR insulator surface under the influence of high voltage electric stress. The particle has to change its presence geometrically by considering the difference in number, position, size and pollution type.

The material characteristics and the geometry of water drop is playing the major role in establishing the electrostatic differences, as seen from the electric field and polarization density. Following are the methodology for every case.

2.2. Methodology

2.2.1 Case I: By Comparing Humid Vs Dry air

The drop has been taken at 90° contact angle under the clean condition with high electric stress, this is to make the model more approachable on the initial conditions. The initial shape (hemisphere) and contact angle corresponds to the hydrophobicity of class WC1 under humid air and then it will be compared with dry air boundary conditions. Then governing equations will direct the field distribution in the simulation considering all the material properties with the applied boundary conditions in the electrostatic physics. The meshing is done with high precision, especially at the drop. The stationary solver has been used to solve the equations numerically at every node of the finite element. The dielectric constant of both the dry and

humid air is the same as 1.02. The difference is observed during specifying the material characteristics while selecting them in a software tool for establishing the relation with dry and humid air conditions effects on the electrostatic parameters. The difference could be notified well through the availability of a molar fraction option which comes into existence only in case of humid air which is taken as 1. The relative humidity and condensation are also considered as the input parameters in this case.

2.2.2 Case II: By Changing Drop Volume

In this case, the representation of volume is taken by area of the hemisphere because this simulation is being performed on a 2D space dimension model. Increasing volume at 90° contact angle in 3D is same as increasing the area at a contact angle of 90°. The geometry, in this case, has been designed with the perfect hemisphere water drop at area of 2094.4 mm^3 and at 7069 mm^3 respectively. Figure 2.1 shows the simulation setup used in this project, the geometry has two aluminium electrode of length 160mm and 10mm in breadth. The SIR insulator slab is modelled with 120mm length and 80 mm breadth, the volume of water drop is assumed to be at 2094.4 mm^3 and 7069 mm^3.

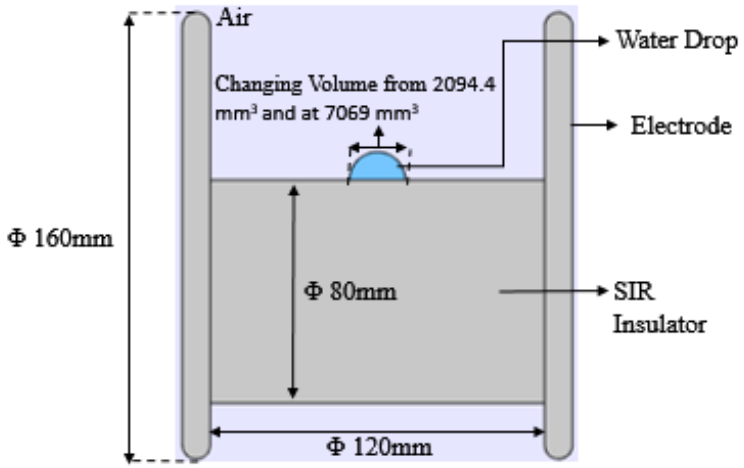

Figure 2.1: Geometry used in this simulation setup

2.2.3 Case III: By Changing the Contact Angle

In figure 2.2 the simulation has been performed on two values of the contact angle at 30° degree and at 120° (In simulation both axes is on the meter scale). The contact angle between the SIR insulator surface and water drop has its impact on the field calculation. The geometry of the drop changed as the contact angle increased this bring the significant difference in the intensification of the field at the edge.

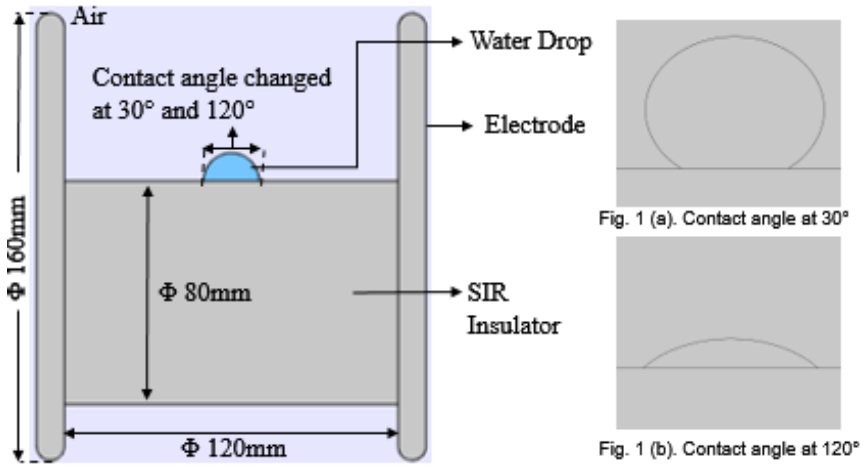

Figure 2.2: Geometric representation for measuring contact angle.

2.2.4 Case IV: By Changing Dust Dielectric Constant

In figure 2.3 the simulation has been performed on two values of the relative permittivity was considered at 2 and 3 respectively. The diameter is kept constant at 5 mm, the contact angle is fixed at 90° and the pollution layer thickness is taken at 1 mm. Here the difference in numerical calculation of field is guided by the increasing relative permittivity of the two dust material only.

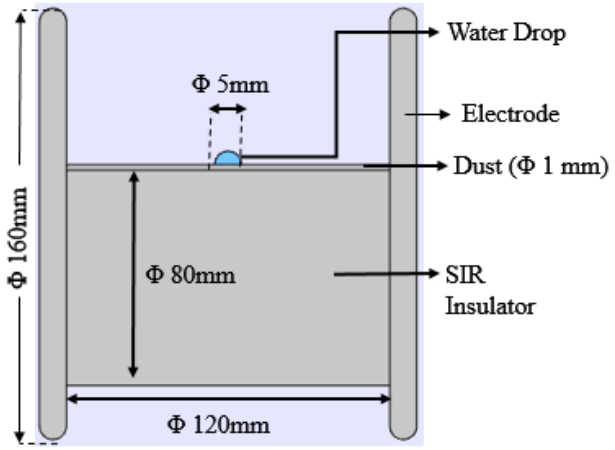

Figure 2.3: Geometric representation for water drop on pollution layer

2.2.5 Case V: Effect of particle presence near TPJ.

Figure 2.4 shows the simulation setup used for this case, the geometry includes two rounded electrode of length 160 mm and 10mm in breadth. The SIR insulator slab is modelled with 120 mm length, 80 mm breadth and particle of 180 μm.

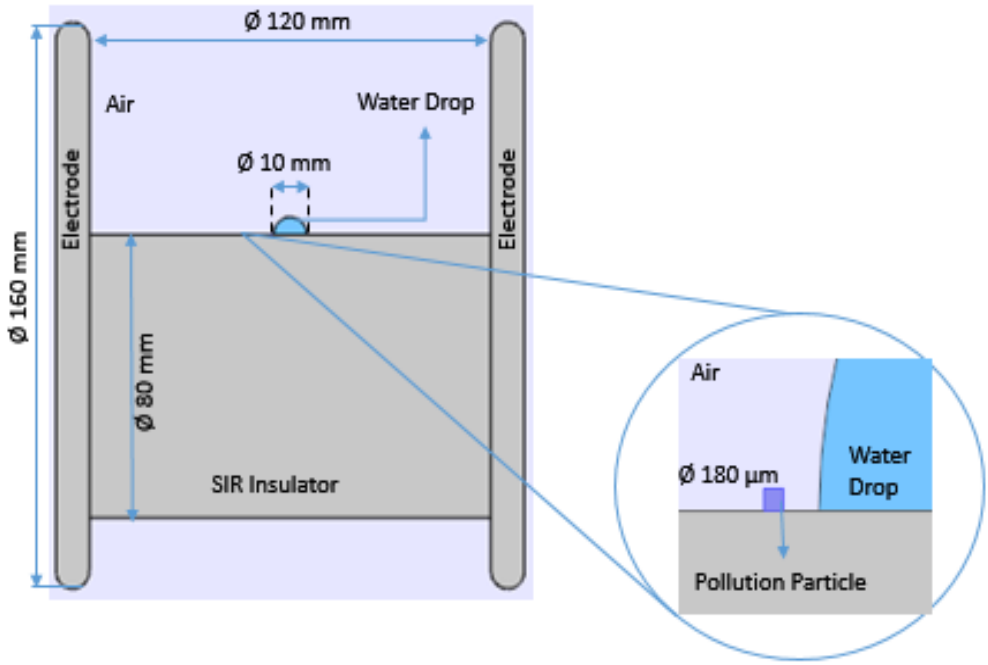

Figure 2.4: Geometric setup used for showing particle presence near water drop

- **Case V-A: Effect of moving the particle closer to TPJ on TPJ:**

The first simulation has been performed only for water drop, then considering a particle of size 180 micrometre which is 2 mm apart from TPJ then 0.5 mm.

- **Case V-B: Effect of increasing the relative permittivity of a particle on TPJ**:

Considering the fact that from dry slat to humid salt particles near the coastal area and the dry sand to saturated sand in the city area, all relative permittivity lies in the range from 4 to 32. So the simulation has been first performed for 12 then followed by 30. During this simulation case, the particle size is remaining constant at 180 micrometres and 1mm apart from TPJ.

- **Case V-C: - Effect of increasing number of a particle on TPJ:**

First the simulation has performed by considering two particles then five. During this the particle size remains constant at 180 micrometres, 1mm apart from TPJ and 1 mm apart to each other.

- **Case V-D: - Effect of increasing the size of particle on TPJ:**

First the simulation was performed by considering the particle size of 60 micrometres then increased to 300 micrometres. During this case of simulation, the particle is 1 mm apart from TPJ.

The reason behind choosing this geometry in all cases, is based on the knowledge that there are two kinds of location for the drop, one is pedant on the insulator shed which is facing horizontal electric field and second is clinging drops on the core which is mostly under vertical electrical field region. Here the investigation is for drop pedant over the insulator shed, so this geometry is natural choice

2.3 Simulation workflow

This simulation has been performed on finite element method software COMSOL Multiphysics. The first step is to make geometry building which has a specific methodology to perform as described in the above section. The parameters are defined as global or local, depending on the need of the problem and addition of physics. The FEMLAB simulation software used to solve every given problem, as shown in the flowchart in figure 2.5.

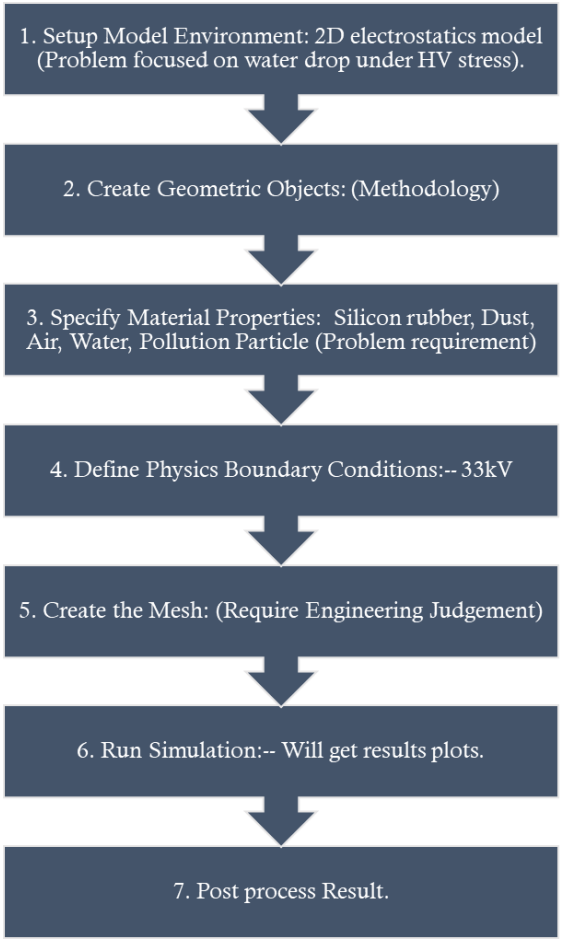

Figure 2.5: Flow chart of FEMLAB simulation

- **Model Environment**

This simulation work has implemented in two dimensions in 2D space dimension, then electrostatic physics in AC/DC module. The study type is stationary because in this study the selected distribution is not dependent on time. This study doesn't need transient time

study or conductive study. Figure 2.6 shows the screenshot of the process to setup model environment window for 2D electrostatic model.

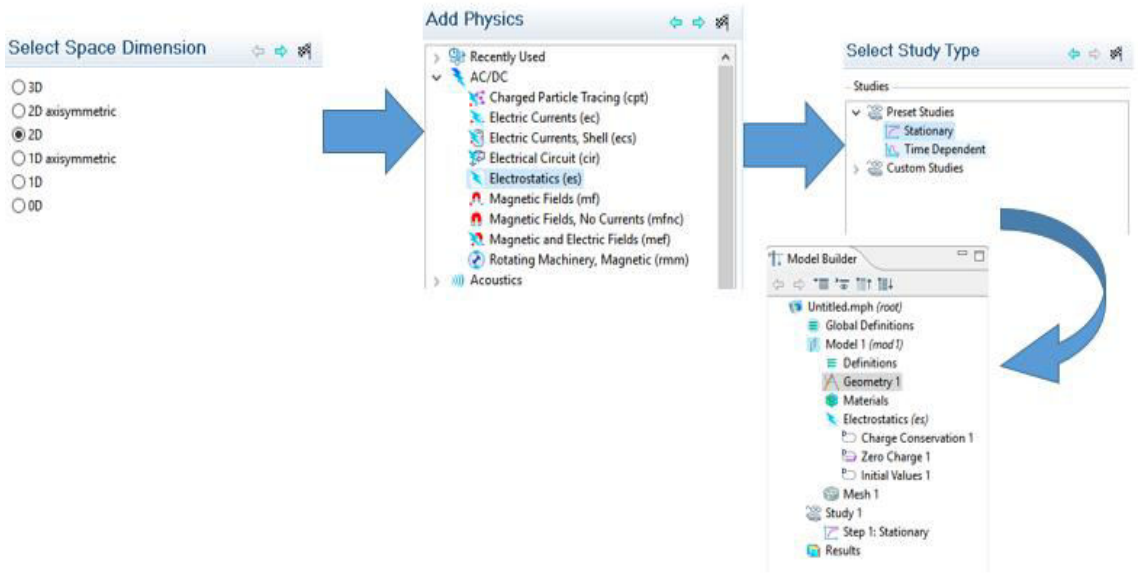

Figure 2.6: Screenshot of the setup model window for 2D electrostatic model.

- **Create Geometry Building**

  Major part of this has already been discussed in methodology section

- **Material Characteristics**

The dielectric constant assigned to air, water drop, electrode, SIR as 1.02,81,1,4.3 respectively to all material as shown in Figure 2.7.

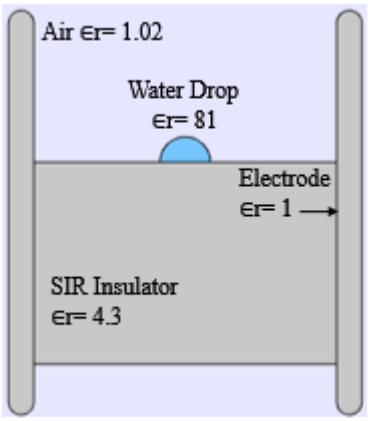

Figure 2.7: Material relative permittivity assigned to SIR insulator, air, water and aluminium

- **Field Equations used.**

This is an electrostatic problem in the static domain because here everything is guided by the relative permittivity of the materials and fixed geometry of the drop. However, there will be a small discharge current starts to flow in case of increasing contact angle but it has been ignored, as it will be of very small value. In this electro hydrodynamic study, magnetic induction and all dynamic current are not involved.

The electrostatic filed simulator solves these equations as taken from [35]

$$\nabla . V = E \quad (1)$$

and Maxwell's equations as

$$\nabla . D = \rho \quad (2)$$

$$D = \varepsilon E \quad (3)$$

By using Equation 2 in 3, we get Poisson's equation as

$$-\nabla . (\varepsilon \nabla . V) = \rho \quad (4)$$

where ε is the relative permittivity of the material, ρ is the space charge density and D is electric flux density used to calculate the polarization flux density in the simulation model. There is no space charge considered in this study hence we put ρ=0, applying this to Equation (4) we get, is the Laplace equation expressed in equation (5)

$$\nabla^2 V = 0 \quad (5)$$

- **Defining Boundary Conditions**

In AC/DC electrostatics physics, five significant boundary conditions are considered for simulation. Those are charge conservation, zero charge, initial values, electric potential and ground boundaries. The charge conservation is assigned to all five domains after that zero charge applicable to both air boundaries by governing equation

$$n . D = 0 \quad (6)$$

Initial boundary condition values applicable to all five domain of the model at voltage zero. In figure 2, high voltage of the order of 33kV is impressed on left-hand side aluminium electrode, where the right-hand side aluminium terminal (electrode) domain is grounded. This is all about boundary conditions assigned to the simulation model. Figure 2.8 shows the screenshot of the setup model window for defining physics boundary conditions in the electrostatic model.

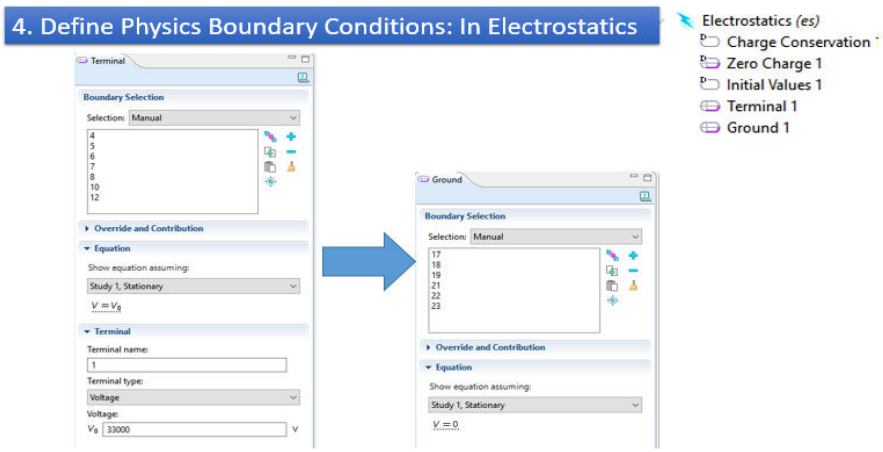

Figure 2.8: Screenshot of the setup window for defining physics boundary conditions

- **Meshing.**

The meshing has been done with precision in both cases of the investigation simulation model. In both cases, the maximum element size value has been taken 0.0025 m where the value of minimum element size has been taken as 5×10^{-6} m. Maximum element growth rate as 1.1, where the value of resolution of curvature taken as 0.2. All these values have applied to all five domains of model the air, water, SIR insulator and aluminium electrode. For meshing two kinds of element shape have been used in the model, first the triangular mesh and the quadrant. Triangular shape has applied to water and dust and remaining all assigned with quadrant shaper.

2.4 Results and Discussion

The results have been obtained through the stationary solver configuration which has compiled the whole simulation model after pre-processing part. Results show the three investigating electrostatic parameters viz. the potential, electric field and polarization density. The focus of the investigation is on the drop because this is the most critical area subjected to electrostatic effects under changing martial characteristic of dry and humid air selection and changing volume.

In case of dry and humid air conditions, simulation results show the potential distribution of water drop at 90° contact angle in both dry and humid air conditions. Figure 2.9 and figure 2.10 show the potential distribution under dry and humid air conditions, respectively. Results show that potential distribution is not much affected by the dry and humid air conditions.

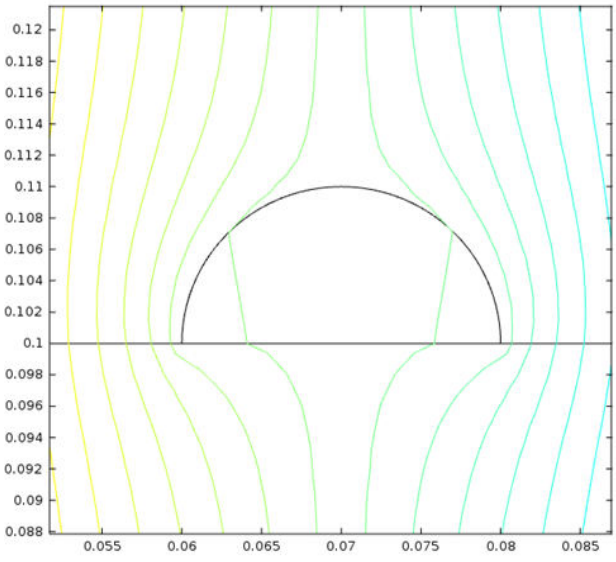

Figure 2.9: Potential distribution contour lines focusing on water drop under dry air condition

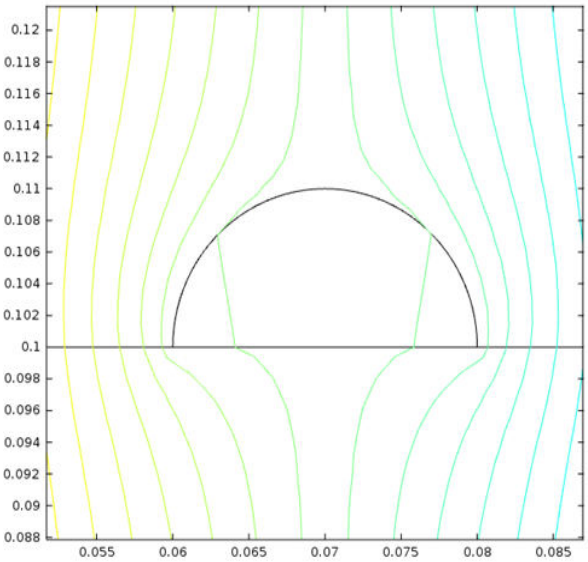

Figure 2.10: Potential distribution contour lines focusing water drop under humid air conditions

The normalized electric field (E-norm) at the triple point of the dry air is numerically found to be 6.2347×10^5 V/m in figure 2.11 where it is 8.1457×10^5 V/m in humid air in figure 2.12. E-norm at the triple junction ends is increased by 23% which is 1.3 times high in the humid air in comparison with dry air.

There is the significant increment at the triple point junction of the water drop in case of humid air. The point to be noted here is that the electric field strength increased without any kind of deformation in the geometry of the drop at 90° contact angle with clean conditions. In humid air conditions, the PD inception voltage is decreasing as proposed by S. Feier-Iova et.al [14] where the electric stress is increasing, will, in turn, decrease the breakdown field strength. Humid air has made it more susceptible to electric break down of drop with an avalanche of electrons flow in small streamers of charged water droplets.

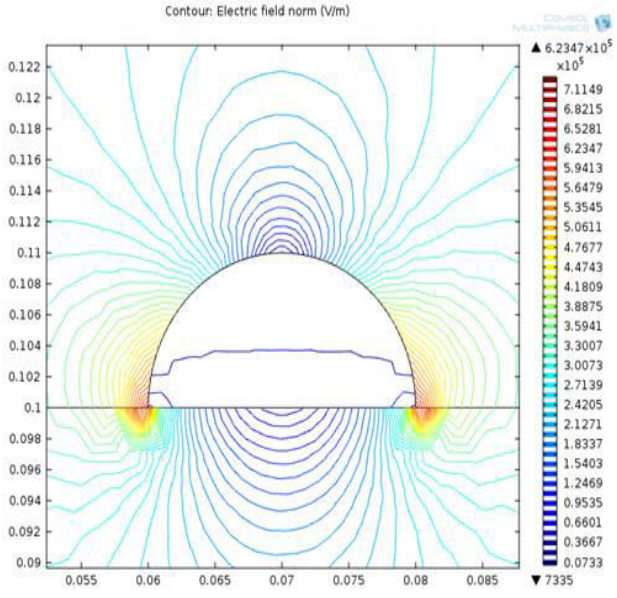

Figure 2.11: E-norm contour lines focusing on water drop under dry air

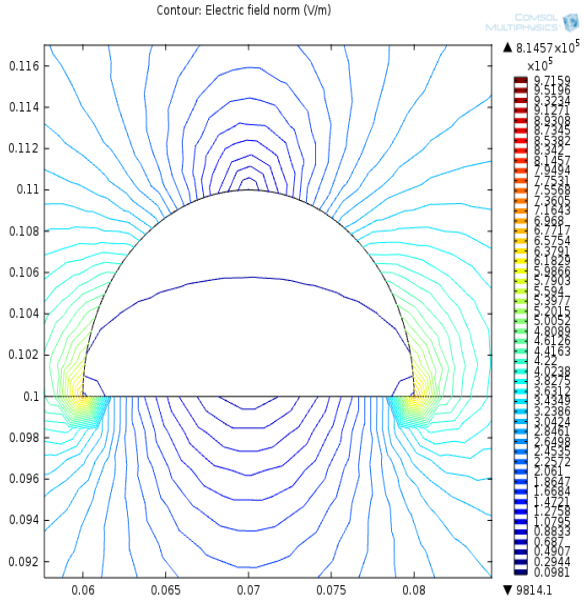

Figure 2.12: E-norm contour lines focusing on water drop under humid air

The cause of deformation in a drop is due to the movement of water droplet along with the electric field distribution pattern, the movement is the effect of the force on the electric dipoles per unit volume. It is seen in both of the cases under dry and humid air conditions are that the strongest dipole moment per unit volume is at the ends of the droplet. Increasing from the centre of a drop to the triple point junction of the water drop.

Figure 2.13 shows that the value of P-norm in dry air condition is 5.8969×10^{-5} C/m^2 and in humid it is 6.5101×10^{-5} C/m^2 in figure 2.14. On comparing humid with dry air conditions, results show that P-norm in humid air condition has been increased significantly by 9.42% or by the factor of 1.10.

In correlation with the concentration of electric field enhancement at the ends, polarization is also seen concentrated at the ends of the drop which can be easily seen in both of the figure 2.13 and figure 2.14 under dry and humid surface plot respectively

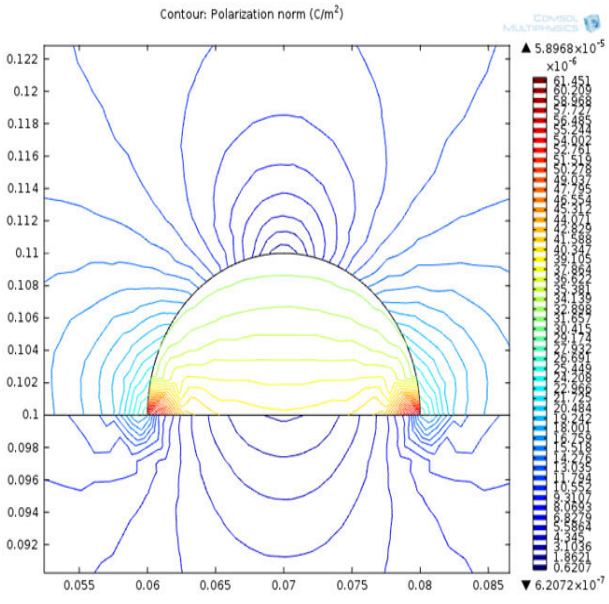

Figure 2.13: P-norm contour lines focusing on water drop under dry air

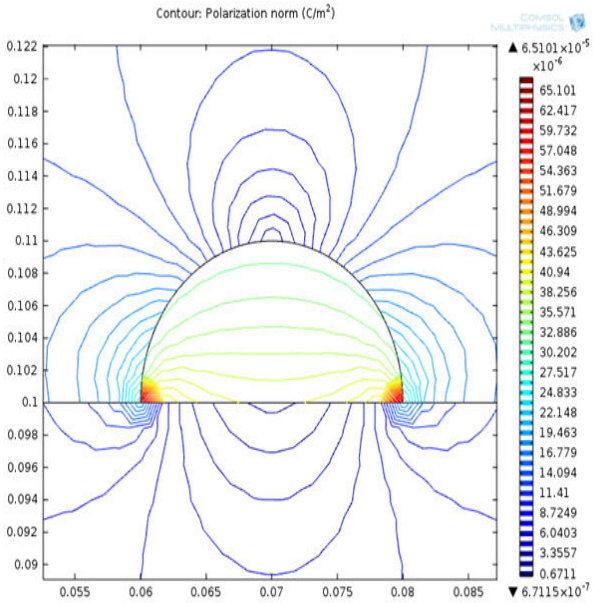

Figure 2.14: P-norm contour lines focusing on water drop under humid air

The increasing electric field intensity increases the polarization charge, thus causing the force field to increase. The results of this also support the fact noticed by C. Song et.al [36] that deformation and elongation of drop increase with the increase in electric field intensity. The local field enhancement accelerates the drop motion velocity hence the degree of deformation increases which in turn related to all PD activities enhancement. In humid air conditions, all polarization and discharge phenomenon is faster than in comparison with dry conditions.

From the above analysis, it is shown that electric field strength and polarization density are closely interlinked in such a way that they both concentrate at the triple point junction of the water, which further leads to exponential increase in polarization and electric stress at the triple point. Then with the degree of deformation as also suggested by other researchers in [36].

Additionally, the value of electric field intensity and polarization density in humid air is increased by 1.3 and 1.10 times respectively as seen from our simulation results compared to dry air at the very initial level of investigation. From this results, It has inferred that the water drop's triple point junction is highly susceptible to all kinds of electrostatic physics occurring under high voltage stress. Under excessive electric potential the droplet can easily breakdown (though it is subjected to further investigation).

In case of volume, we are increasing the volume from 2094.4 mm^3 to 7069 mm^3 by increasing the diameter of the water drop from 10 mm to 15 mm. The increment in the diameter with 5 mm will reflect back to the increment in volume of the water drop. The E-norm at the triple point junction when volume is 2094.4 mm^3 is numerically found to be 1.088×10^6 V/m in figure 2.15 where it is 1.2017×10^6 V/m when volume is 7069 mm^3 in figure 2.16. E-norm at the triple point junction is increased by 10.45% as volume is increasing.

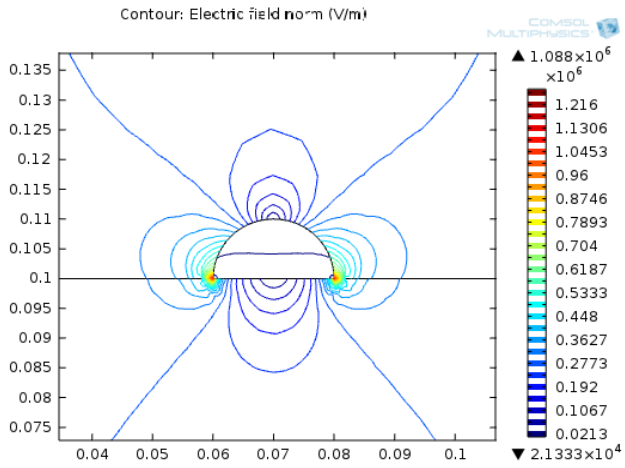

Figure 2.15: E-norm contour lines focusing on water drop at volume of 2094.4 mm^3

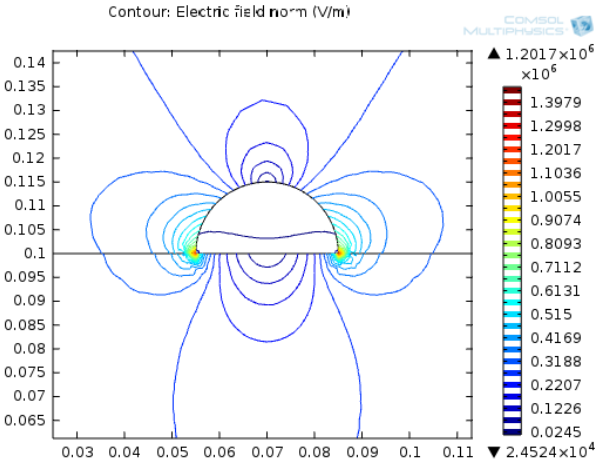

Figure 2.16: E-norm contour lines focusing on water drop at volume of 7069 mm^3

The P-norm at the triple point junction when volume is 2094.4 mm^3 is numerically found to be 6.3852×10^{-5} V/m in figure 2.17 where it is 6.7593×10^{-5} V/m when volume is 7069 mm^3 in figure 2.18. E-norm at the triple point junction is increased by 5.85% as volume is increasing.

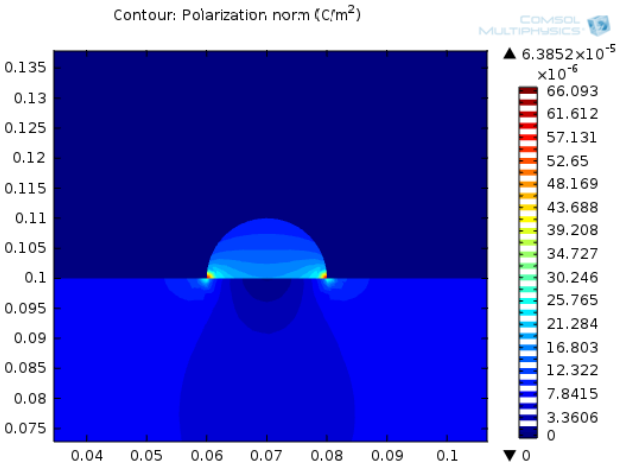

Figure 2.17: P-norm contour lines focusing on water drop when volume at 2094.4 mm^3

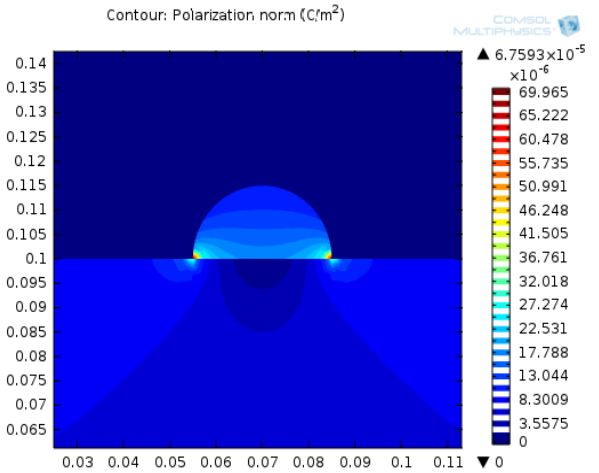

Figure 2.18: P-norm contour lines focusing on water drop when volume at 7069 mm^3

The comparison of E-norm and P-norm in both cases in depicted in table 2.1. Table 2.1 is showing two comparing quantities first the incremental percentage and second the incremental factor of the normalized electric field and normalized polarization density

respectively during humid air with respect to dry air. E-norm increased by 23.4% where P-norm by 9.42% during humid air condition as mentioned in the table. Other quantity increment factor in E-norm which has increased by 1.3 where P-norm by 1.10 times of the dry air. This is the significant increment in the electrostatic quantities during humid air in comparison with dry air conditions.

TABLE 2.1. PERCENTAGE INCREMENT OF E-NORM AND P-NORM IN CASE I AND CASE II

S.No	**Increment in normalized electric field and polarization density during humid air in comparison with dry air.**		
	Comparing Quantities	***E-norm***	***P-norm***
1.	By Comparing Humid Vs Dry air	23.4 %	9.42 %
2.	By Changing Drop Volume	10.45 %	5.85 %

In case of changing the contact angle, in figure 2.19 the normalized electric field at triple point junction of 30° contact angle water drop is 1.1704×10^{6} V/m where in 120° contact angle in figure 2.20 it is 1.593×10^{4} V/m. E-norm has increased by 36.10% in 120° contact angle water droplet.

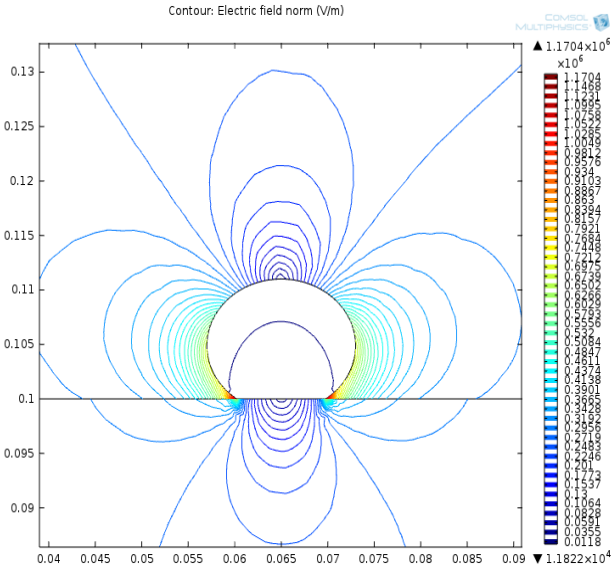

Figure 2.19: E-norm contour lines focusing on water drop at 30° contact angle

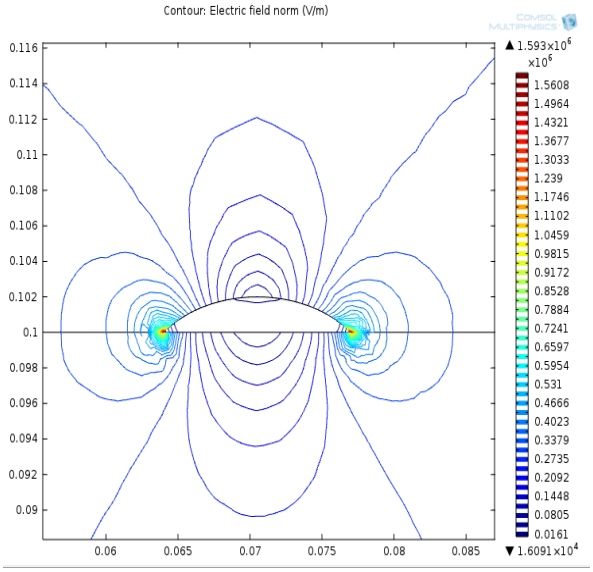

Figure 2.20: E-norm contour lines focusing water drop at 120° contact angle

In figure 2.21 the normalized polarization density at triple point junction of 30° contact angle water drop is 2.2345×10^{-5} C/m^2 where in 120° contact angle in figure 2.22 it is 8.8544×10^{-5} C/m^2.P-norm has increased by 296.25% in 120° contact angle water drop.

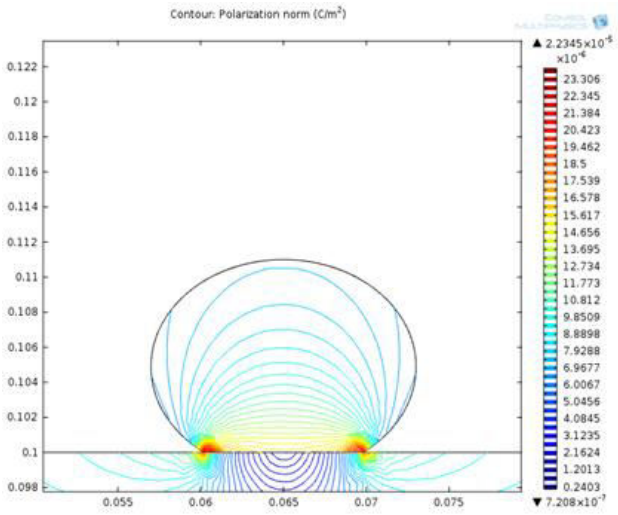

Figure 2.21: P-norm contour lines focusing on water drop at 30° contact angle.

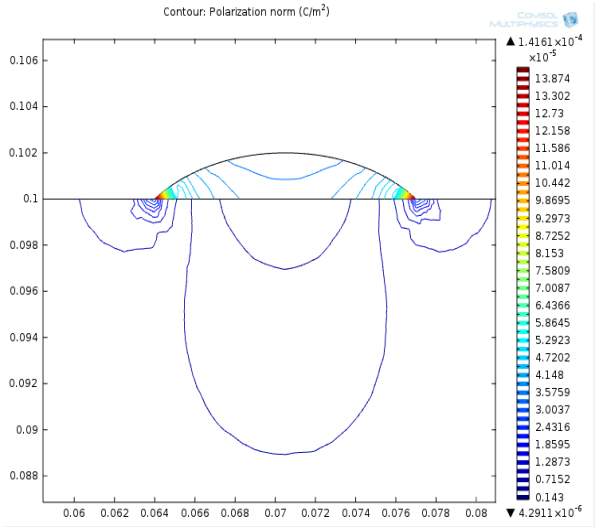

Figure 2.22: P-norm contour lines focusing water drop at 120° contact angle.

In case of changing the dust relative permittivity, figure 2.23 shows the normalized electric field at triple point junction of silica dust water drop is 1.1259×10^{6} V/m where in urea dust in figure 2.24 it is 1.2227×10^{6} V/m. E-norm has increased by 1.186% in case of urea dust,which have dielectric constant of 3.

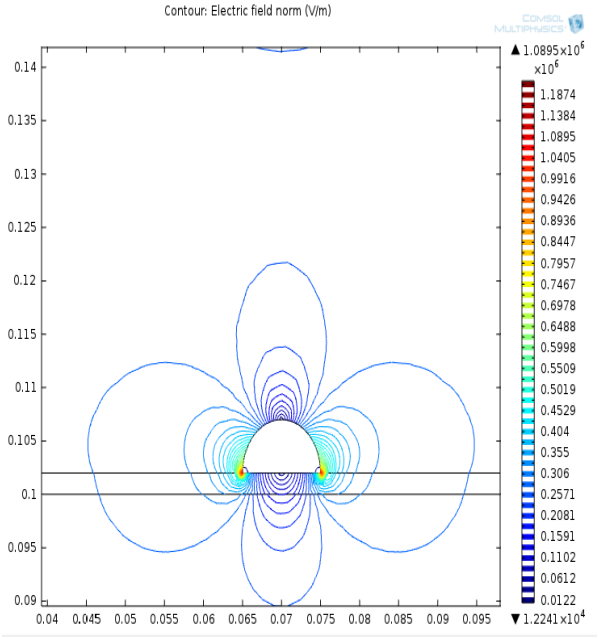

Figure 2.23: E-norm contour lines focusing on water drop under silica dust

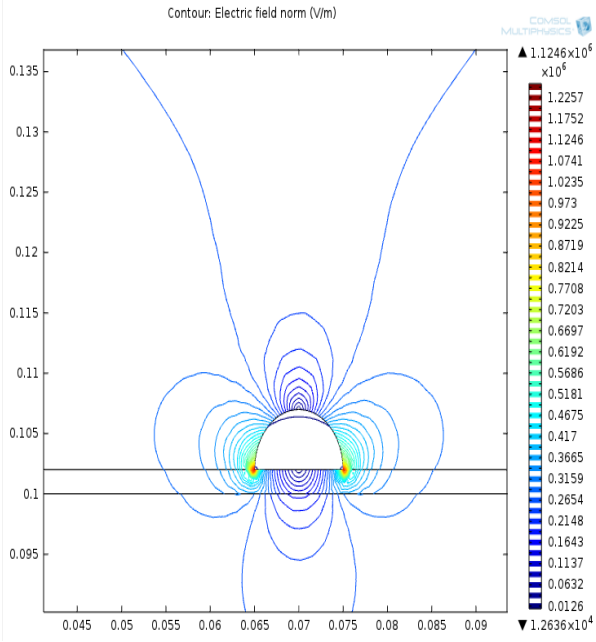

Figure 2.24: E-norm contour lines focusing on water drop under urea dust.

The polarization density in figure 2.25 the normalized polarization density at triple point junction of silica dust (ε_r =2) is 3.2637×10^{-5} C/m^2 where urea dust in figure 2.26 it is 4.3349×10^{-5} C/m^2. P-norm has increased by 32.82% in case of urea dust, which have dielectric constant of 3

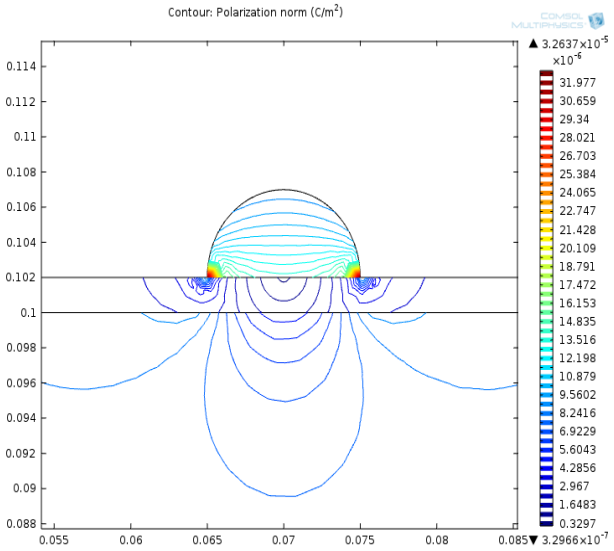

Figure 2.25: P-norm contour lines focusing on water drop under silica dust

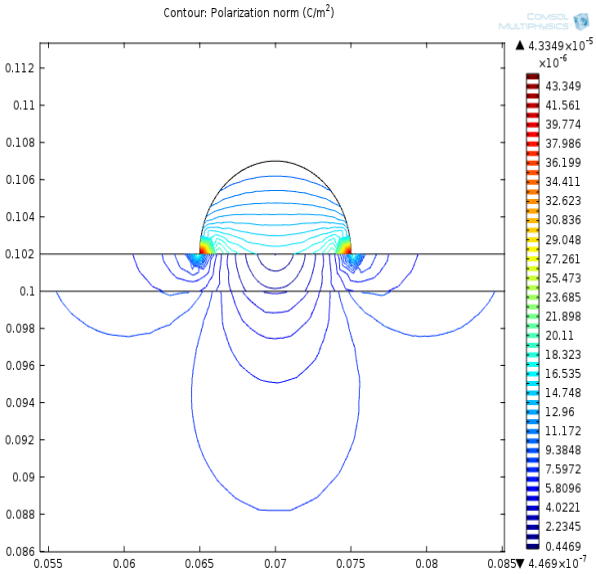

Figure 2.26: P-norm contour lines focusing on water drop under urea dust

Table 2.2 is shows two investigating parameters in both of the cases, first investigating parameter is the E-norm incremental percentage at the triple point junction of the drop in 120° contact angle with respect to the triple point junction of 30° contact angle, which is 36.10%. Similarly, in case III the E-norm incremental percentage at the triple point junction in silica dust with respect to the urea dust is 1.118%. The second investigating parameter is P-norm incremental percentage at the triple point junction of the drop in 120° contact angle with respect to the triple point junction of 30° contact angle, which is 296.25%. Similarly, in case III the P-norm incremental percentage at the triple point junction in silica dust with respect to the urea dust is 32.82%.

TABLE 2.2. INCREMENT OF E-NORM AND P-NORM IN CASE III AND CASE IV

S.No	**Increment in normalized electric field and polarization density during case III and case IV**		
	Cases	***E-norm in %***	***P-norm in %***
1.	Case III. Contact angle	36.10	296.25
2.	Case IV. Dust dielctric constant	1.118	32.82

Table 2.3 shows two investigating parameters in both of the cases, first is the ratio between maximum E-norm at the triple point to the applied electric field (275000 V/m) called as E-norm enhancement ratio. The second investigation parameter is the increased value of P-norm at the triple point with respect to the value of P-norm at the middle of the water drop called as P-norm intensification percentage. E-norm enhancement ratio in 30° contact angle of case I is

4.25 times where in 120° contact angle it is 5.8 times. In case II the E-norm enhancement ratio in silica dust is 4.09 times where in case of urea dust it 4.46 times. P-norm intensification percentage in 30° contact angle of case I is 52.36% where in 120° contact angle it is 297.59% or approximately 3 times. In case II P-norm intensification percentage in silica dust is 147.63% where in case of urea dust it 174.56%.

TABLE 2.3. E-NORM ENHANCEMENT RATIO AND P-NORM INTENSIFICATION % IN CASE III AND IV

S.No	Increment in normalized electric field and polarization density during case III and case IV		
	Specific Cases	**E-norm Enhancement Ratio**	**P-norm intensification %**
1.	Case III.A. Contact angle at 30°	4.256	52.36
2.	Case III.B .Contact angle at 120°	5.79	297.59
3.	Case IV.A. Silica dust at $\varepsilon_r = 2$	4.094	147.63
4.	Case IV.B. Urea dust at $\varepsilon_r = 3$	4.4618	174.56

In case of particle presence, figure 2.27 and figure 2.28 shows electric field and polarization density when no particle is present to influence the TPJ which is 9.7448×10^{5} V/m and 5.8384×10^{-5} C/m^2 respectively where when one particle is present the electric field and polarization density is 1.534×10^{6} V/m and 9.2758×10^{-5} C/m^2 shown in figure 2.29 and figure 2.31 respectively. Hence, the significant amount of increment is clearly seen in both the electric field and polarization density which showed the effect of the presence of a particle on TPJ.

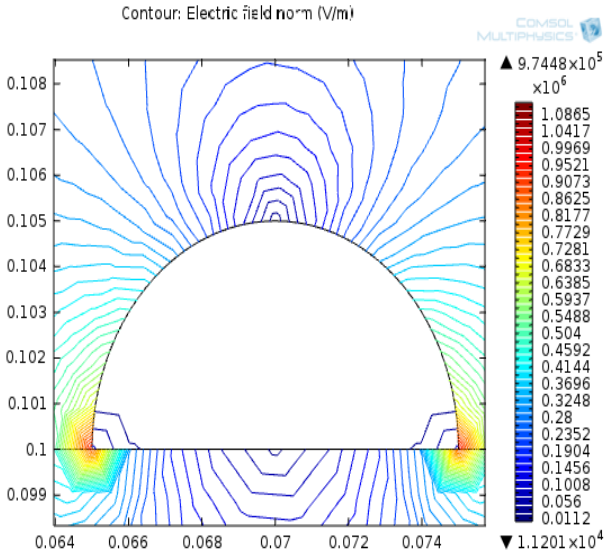

Figure 2.27: Electric field around water drop in absence of particle.

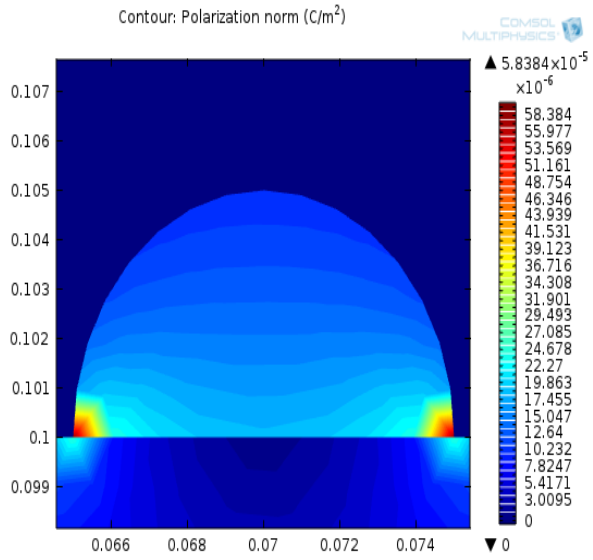

Figure 2.28: Polarization density around water drop in absence of particle.

In case of decreasing the distance of particle from TPJ of the water drop, figure 2.29 shows the normalized electric field at TPJ when the particle is 2 mm away from TPJ is 1.534×10^{6} V/m, where when the distance has been decreased to 0.5 mm away from TPJ in figure 2.30. E-norm is 1.962×10^{6} V/m. So, E-norm has been increased by 27.9 %. As the particle is moving closer to the water drop TPJ, the E-norm at TPJ is increasing.

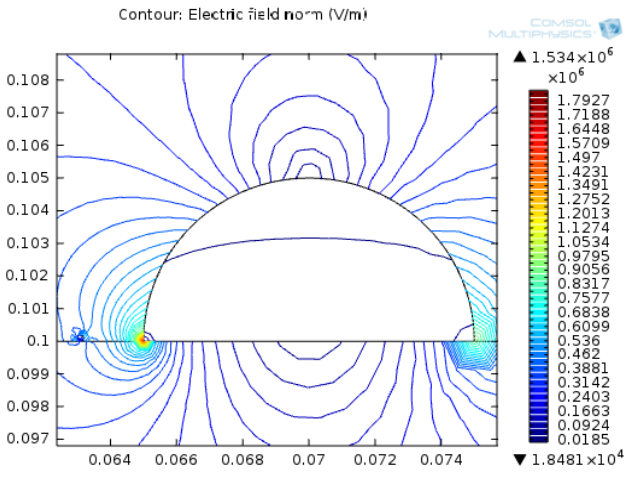

Figure 2.29: E-norm contour lines when particle is present 2 mm away from TPJ from left.

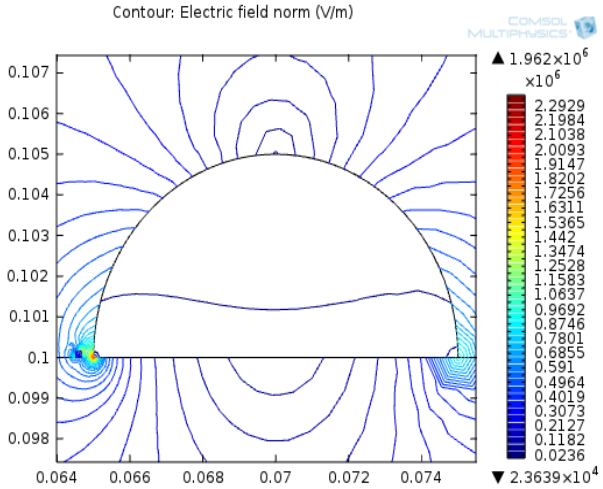

Figure 2.30: E-norm contour lines when particle is present 0.5 mm away from TPJ from left.

The polarization density as in figure 2.31 the P-norm at TPJ when the particle is 2 mm away from TPJ is 9.2758×10^{-5} C/m^2, where when the distance has been decreased to 0.5 mm away from TPJ in figure 2.32. P-norm is 1.2408×10-^{4} C/m^2. So P-norm has been increased by 33.76 %. As the particle is moving closer to the water drop TPJ, the P-norm at TPJ is increasing.

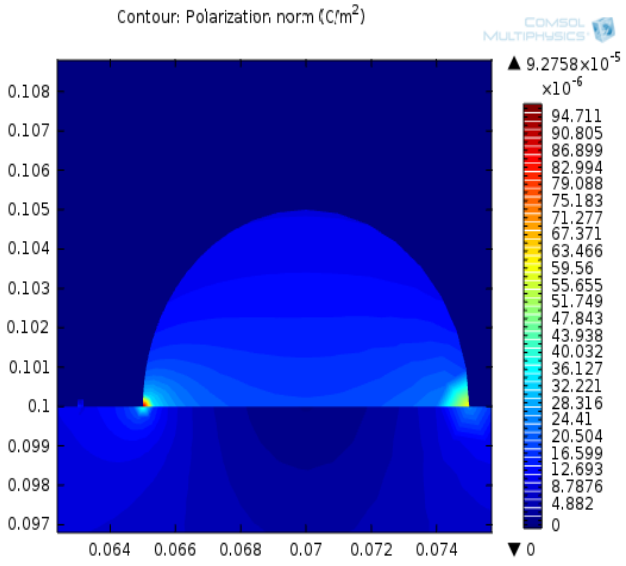

Figure 2.31: P-norm contour lines when particle is present 2 mm away from TPJ from left.

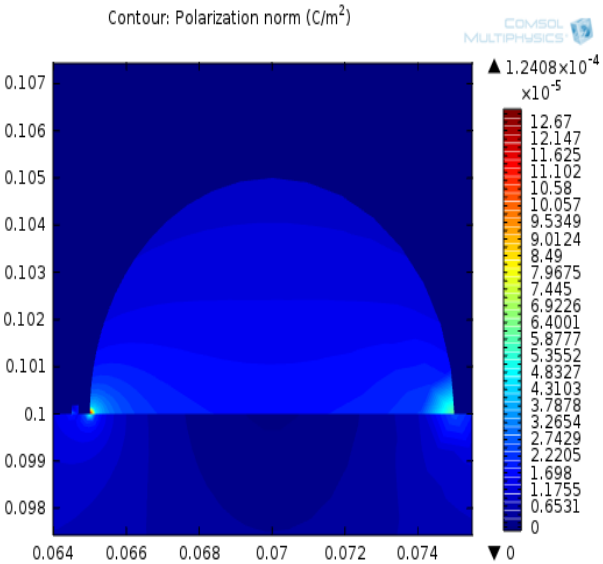

Figure 2.32: P-norm contour lines when particle is present 0.5 mm away from TPJ from left.

In case of increasing relative permittivity of a particle near TPJ of a water drop, in figure 2.33 the E-norm at TPJ when the particle has a relative permittivity of 12 is 1.707×10^6 V/m, where when the relative permittivity has been increased to 30 in figure 2.34. E-norm is 1.7084×10^6 V/m. So E-norm has been increased by 0.08 %. As particle relative permittivity has been increasing, the E-norm at TPJ is increasing very insignificantly. The particle size is remaining constant at 180 micrometers, 1mm apart from TPJ.

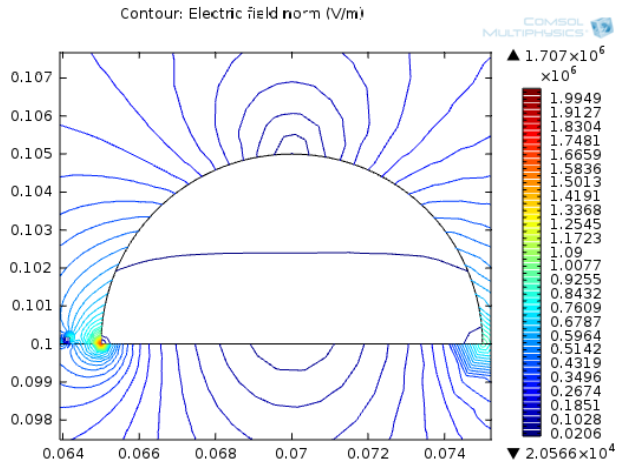

Figure 2.33: E-norm contour lines when particle of relative permittivity 12 is present

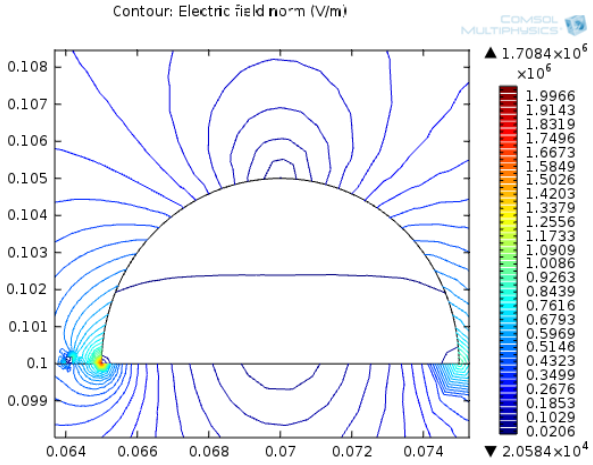

Figure 2.34: E-norm contour lines when particle of relative permittivity 30 is present

In figure 2.35 the P-norm at TPJ when the particle has a relative permittivity of 12 is 1.061×10^{-4} C/m^2, where when the distance has been increased to 30 in figure 2.36 E-norm is 1.0618×10^{-4} C/m^2.So P-norm has been increased by 0.07 %. As particle relative permittivity has been increasing, the P-norm at TPJ is increasing but very insignificantly. The particle size is remaining constant at 180 micrometres, 1mm apart from TPJ.

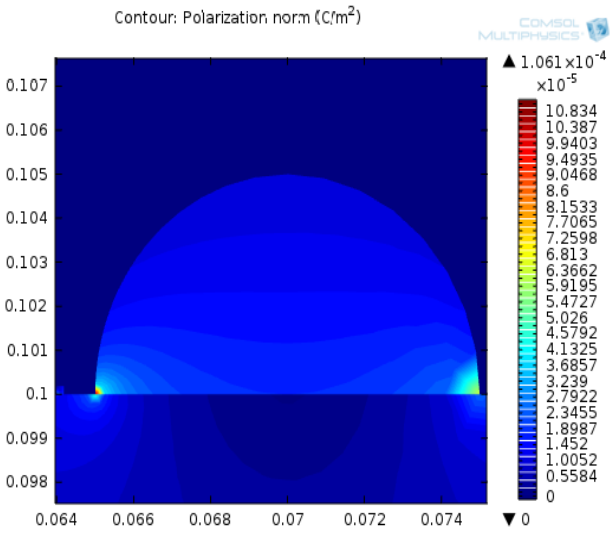

Figure 2.35: P-norm contour lines when particle of relative permittivity 12 is present

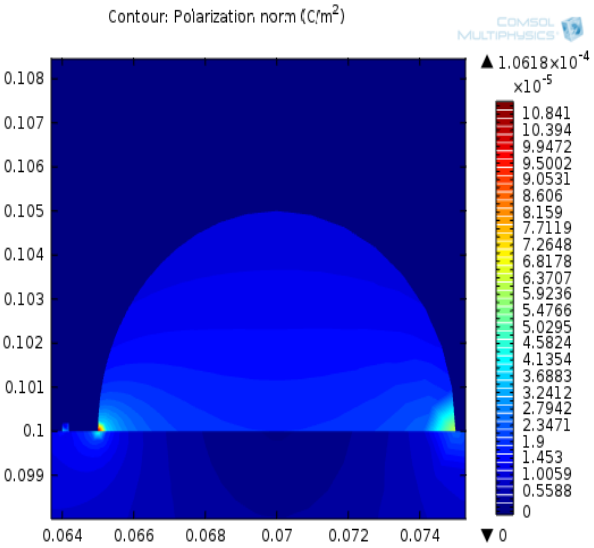

Figure 2.36: P-norm contour lines when particle of relative permittivity 12 is present

In case of effect of increasing number of a particle on TPJ of a water drop, the electric field, First, the simulation was performed by considering two particles then three, the particle size is remaining constant at 180 micrometres, 1mm apart from TPJ and 1 mm apart to each other. In figure 2.37 the E-norm at TPJ when two particle considered is 1.7002×10^{6} V/m, where when the particle has been increased to five in figure 2.38 E-norm is 1.7108×10^{6} V/m. So E-norm has been increased by 0.623 %. As particle has been increasing, the E-norm at TPJ is also increasing. The particle size is remaining constant at 180 micrometres, 1mm apart from TPJ.

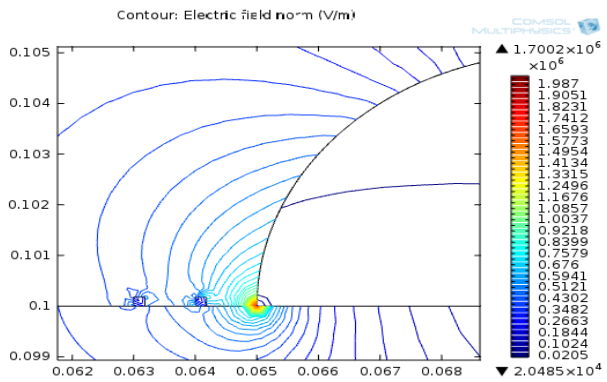

Figure 2.37: E-norm contour lines when two particles are present

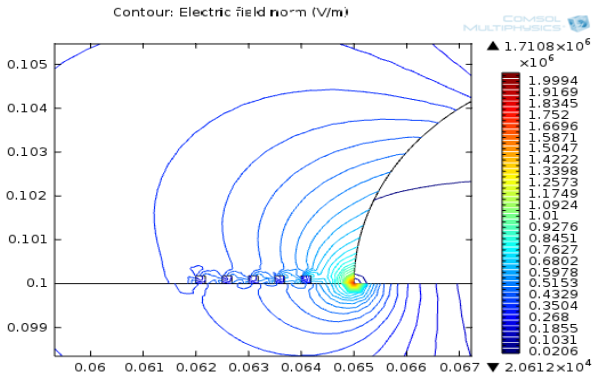

Figure 2.38: E-norm contour lines when five particles are present

In case of effect of increasing number of a particle near TPJ of a water drop, for polarization density, First, the simulation was performed by considering two particles then three, the particle size is remaining constant at 180 micrometres, 1mm apart from TPJ and 1 mm apart to each other. In figure 2.39 the P-norm at TPJ when two particles considered is 1.0523×10^{-4} C/m^2, where when the particle has been increased to five in figure 2.40. E-norm is 1.0547×10^{-4} C/m^2. So P-norm has been increased by 0.22 %. As particle has been increasing, the P-norm at TPJ is also increasing. The particle size is remaining constant at 180 micrometres, 1mm apart from TPJ

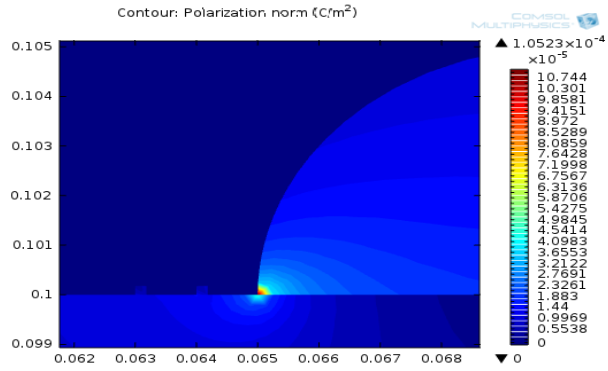

Figure 2.39: P-norm contour lines when two particles are present

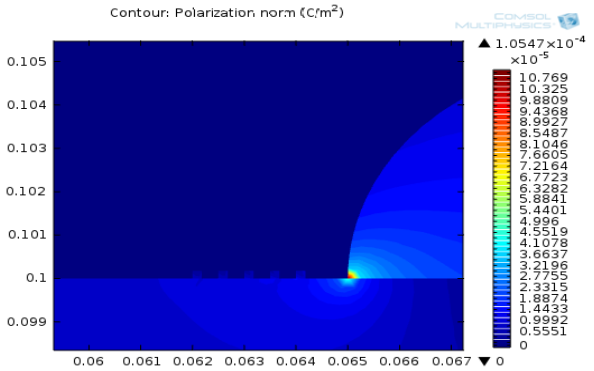

Figure 2.40: P-norm contour lines when five particles are present.

In case of Effect of increasing the size of a particle near TPJ of a water drop, Effect of increasing the size of a particle on TPJ of water drop: First the simulation was performed by considering the particle size of 60 micrometres then increased to 300 micrometres. The particle is 1 mm apart from TPJ. In figure 2.41 the E-norm at TPJ when the particle has a size of 60 µm is 2.1805×10^{6} V/m, where when the particle size has been increased to 300 µm in figure 2.42 E-norm is 1.4264×10^{6} V/m. So E-norm has been decreased by 34.58 %. As particle size has been increasing, the E-norm at TPJ is decreasing.

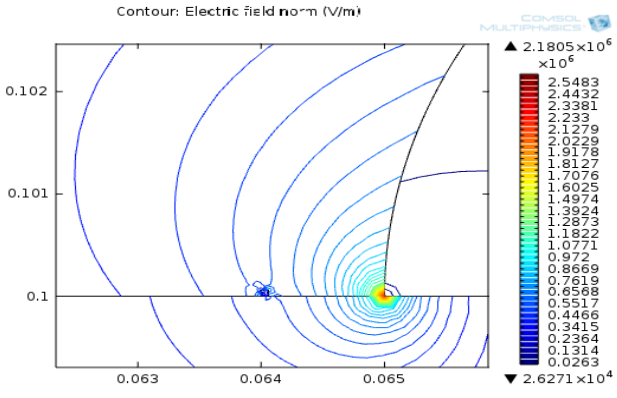

Figure 2.41: E-norm contour lines when particle 60 µm is present.

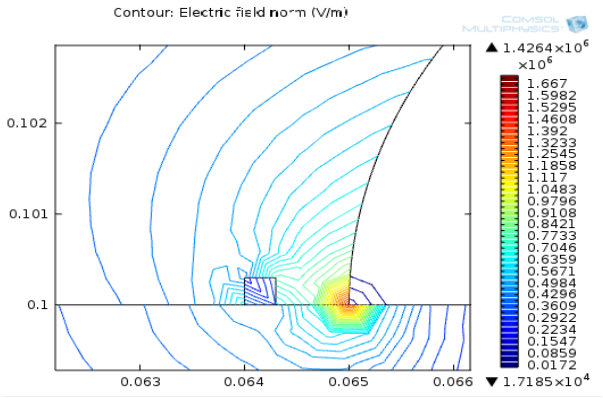

Figure 2.42: E-norm contour lines when particle 300 µm is present.

In case of polarization density Effect of increasing the size of a particle on TPJ of water drop: First the simulation was performed by considering the particle size of 60 micrometres then increased to 300 micrometres. The particle is 1 mm apart from TPJ. In figure 2.43 the E-norm at TPJ when the particle has a size of 60 µm is 1.3389×10-4 C/m2, where when the particle size has been increased to 300 µm in figure 2.44 E-norm is 9.5152×10-5 C/m2. So E-norm has been decreased by 28.93 %. As particle size has been increasing, the P-norm at TPJ is decreasing.

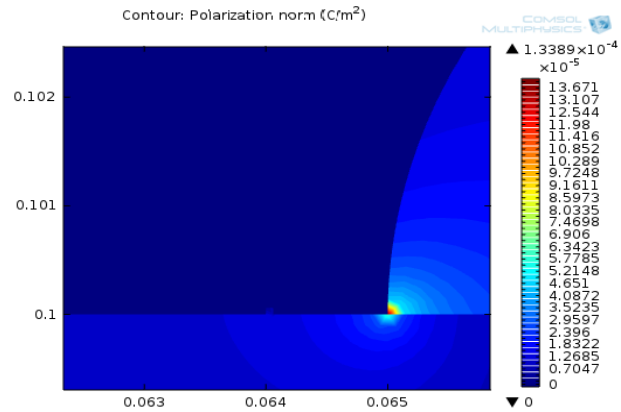

Figure 2.43: P-norm contour lines when particle 60 µm is present.

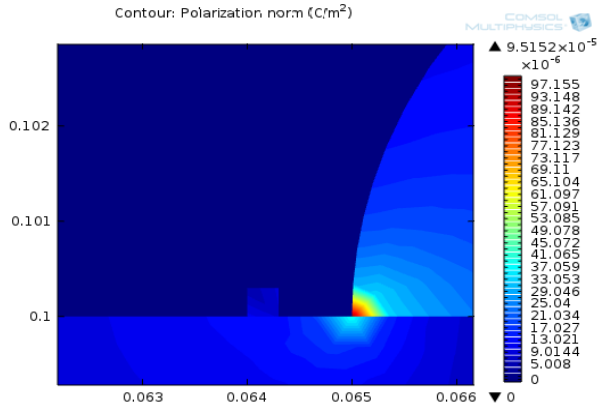

Figure 2.44: E-norm contour lines when particle 300 µm is present.

From Table 2.4 it is clearly inferred that as the particle move closure to the TPJ and size of the particle decreases the electric field and polarization density on TPJ has been increased significantly where the increment in the electric field and polarization density in case of increasing the number of particles and relative permittivity is not a significant increment but the nature is increasing

TABLE 2.4: E-NORM INTENSIFICATION AND P-NORM INTENSIFICATION % FROM THE CASE V-A TO V-B

S.No	**% Increment or decrement in the E-norm and P-norm during all four cases from V-A to V-D**		
	Specific Cases	***E-norm %***	***P-norm %***
1.	Case V-A. Effect of moving particle closer to TPJ on TPJ of water drop	Increased by 27.9 %	Increased by 33.76%
2.	Case V-B Effect of increasing relative permittivity of a particle on TPJ of water drop	Increased by 0.08%	Increased by 0.075%
3.	Case V-C. Effect of increasing number of a particle on TPJ of water drop	Increased by 0.623%	Increased by 0.22%
4.	Case V-D. Effect of increasing the size of a particle on TPJ of water drop	Decreased by 34.58%	Decreased by 28.93%

After analysing every case of the investigation it is clearly seen that at the triple point junction the electric field and polarization density has been shifted from both sides ends of the drop to the left side end where the particle heterogeneity is present. The settled particles deposited over the insulator surface cause distortion in the electric field causes non-uniformity in the distribution which always affect the breakdown voltage such that it reduces which has also been noted by G. Moustafa et. al in [18] during his dust storm investigation in the air. The distorted electric field has a nature to reduce the breakdown voltage between gaps because of its unevenness in the field, visual observation from the investigation showed that unevenness due to the presence of a particle or uneven micrometre settled bumped has increased the electric field on TPJ of a water drop. As the size of the particle or micrometre settled bumped

decrease the electric field and polarization density has increased significantly which has also shown good agreement with the experimental findings by G. Moustafa et. al in [18] during his dust storm investigation between the electrode in the air only. In summary, this dissertation contribution can be used to learn effectively about how the electrostatic parameters at a triple point junction have influenced by the presence of micrometre particle or micrometre settled bumped using the finite element method.

CHAPTER 3

NANO-DIELECTRIC STRENGTH UNDER HIGH VOLTAGE STRESS

3.1 Introduction

In this chapter, interest is to understand the factors which influences the nano composite material. Numerous factors and phenomenon affect the behavior of nano material, which is highly unpredictable, vast, complex and still unknown i.e. nano interface. This work is an attempt to understand a little in the huge-deep knowledge of nano physics. The coming cases are investigated by restricting the effect in many dimensions like neglecting its quantum physics, molecular chemistry, molecular physics, solid state physics etc. Here, in this study the behavior is completely based on the electric field response vs material's permittivity for exploring the interface and nanocomposite behavior, specifically from permittivity perspective. So, simulation has several assumptions for its ease, as follows.

- From geometry particles are spherical.
- Interaction between particle and polymer is strong.
- In base material the distribution of nano filler is homogeneous.
- Normalised electric field is only dependent in relative permittivity.
- No temperature effects are considered.
- Neglecting the presence of space charge density completely.
- The dielectric material is homogeneous.

Now, coming to the cases taken for study are as follows,

- In case first, the effective permittivity of the sample has considered to be increased and analysing its effect on water void. Water void is the initiator of partial discharge in the base insulation material. So, how it behaves in case of nano-composite material is the purpose to see and analyse.
- In case second, the void in the sample can be of ellipsoid shape also, so the effect of change in the electric field near drop by change in shape has been computed and analysed.
- In case third, there is choice in the base insulation material in the market, from low density polythene to high density polythene or from cross linked polythene to epoxy. On the basis of permittivity, what value of permitted will give better insulation. So, by changing the base material what happens in the nano-interface electric filed has been analysed.

- In case forth, from the fact that, nano- particles comes with choices, from lower permittivity value to the rare highest value are available. Investigators use hit and trial method to concluded which nano particle should be used in the base material. So, this case-study is an attempt to solve the mystery, at least from the permittivity. Though, results don't ensure the guarantee because study has several assumptions as mentioned above but this study provide some useful insights as a guide.
- In case fifth, this case is subjected to solve the unknown behaviour of the nano-interface by intentionally giving the permittivity values to the interface.
- In case sixth, as we know by increasing the number of nano-particle the insulation strength increases but huge amount of doping of nano material started to decrease the insulation strength. This case validates this fact by decreasing the inter particle distance through simulation.
- In this last case, seventh case has four sub-cases. A new approach to embed nano particle over other nano particle by a method called electrospinning. With two nano particles of different value we can have four combinations of arranging them in base material. So, here four models in which the nano-particles can be configured has subjected to investigation. The best configuration from the perspective to enhance the dielectric strength has been figured out by this simulation model.

All these cases have been done, by considering the base-line fact that, the good nanocomposite insulator have electric field inside the material on higher side. This fact has been concluded from the experiments after performing a lot of research on materials. It has to be noted that all these investigations are true in their restricted domain only, which do not advocate the true nature of the nano-composite material if they really performed experimentally. This study is exploring the behavior of nano-composites by permittivity only, whose results can be used by future researchers to cross check and as a guide in the judgement to choose the next material. Though the experimentation verification of all these and many different physics studies by simulation has subjected to future work.

3.2 Methodology

3.2.1 Case I: By Changing Sample Permittivity with Water Void Model.

As shown in figure 3.1 nano-composite base of 1mm × 1mm, with water void of 500nm in it, taking this geometry as base model, the relative permittivity has been increased from 10 to 30. So, simulation is first performed for permittivity of value 10 then 30. Figure 3.2 is zoom in picture of that water void inside the material.

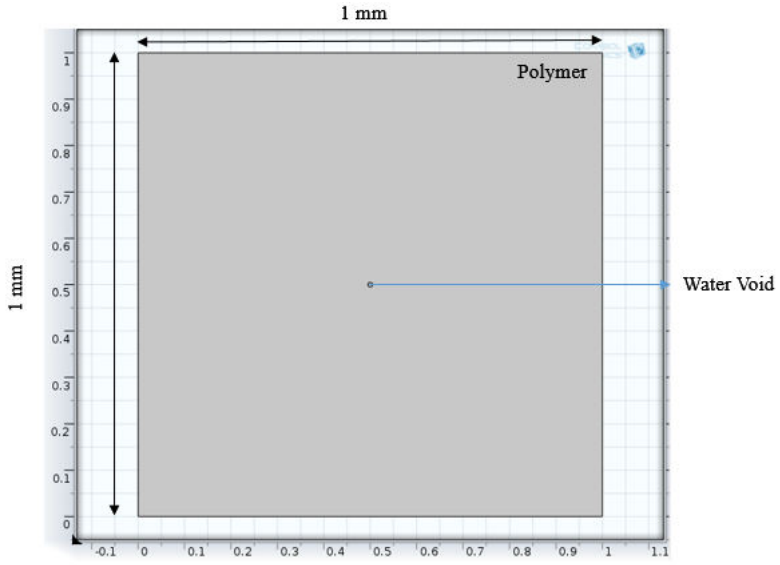

Figure 3.1: Geometry of the water void model

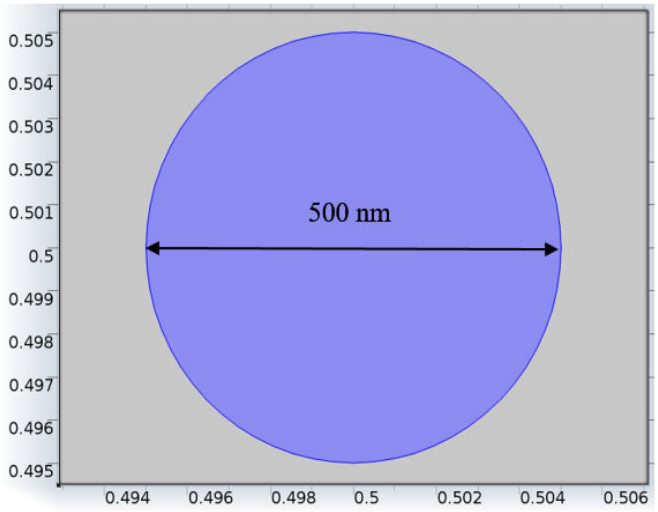

Figure 3.2: Zoom in picture of spherical water void

3.2.2 Case II: By Changing Shape of Water Void.

From the fact that, water void can be of ellipsoid shape also, the spherical water has been replaced in the same 1mm × 1mm nanocomposite with ellipsoid void, as shown in figure 3.3.

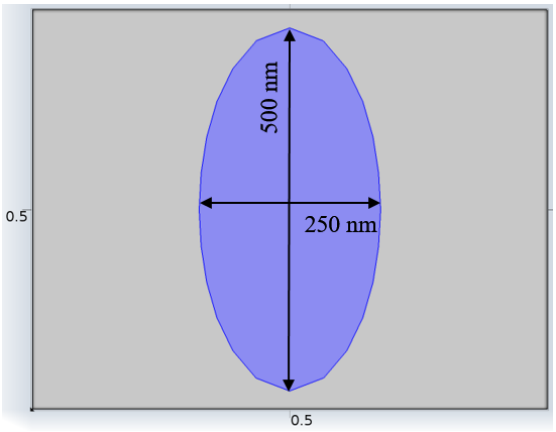

Figure 3.3: Zoom in picture of ellipsoid water void

3.2.3 Case III: By Changing Polymer Material

The base material relative permittivity has been increased from LDPE to epoxy i.e. 2.25 to 3.5. So the simulation has been run for 2.25 then 3.5 as shown in figure 3.4.

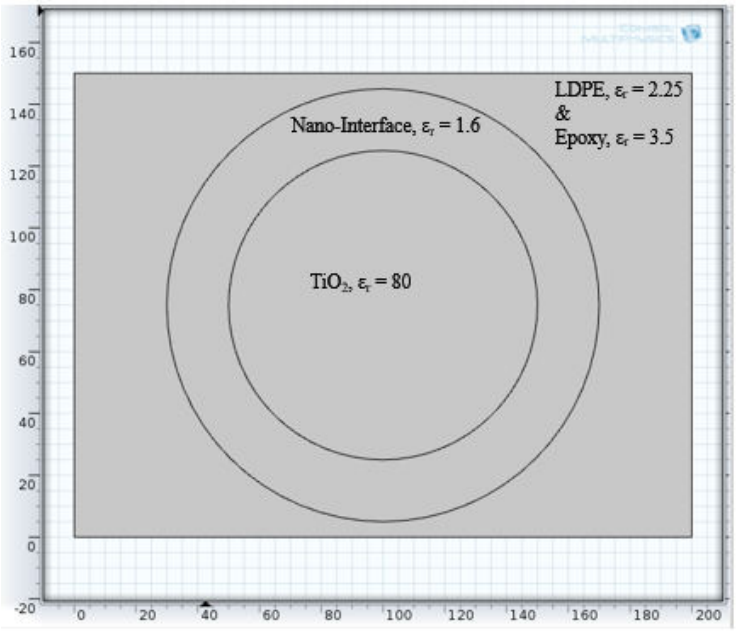

Figure 3.4: Material assigned to changing polymer material model

3.2.4 Case IV: By Changing Nano- Filler Material

In this case, the purpose is to increase the relative permittivity of filler material, so the simulation has been run for Calcium Carbonate nanoparticles which has relative permittivity of 4.5. Then the same model simulation has been run for Barium Titanate nanoparticles which have relative permittivity of 170 as shown in figure 3. 5.

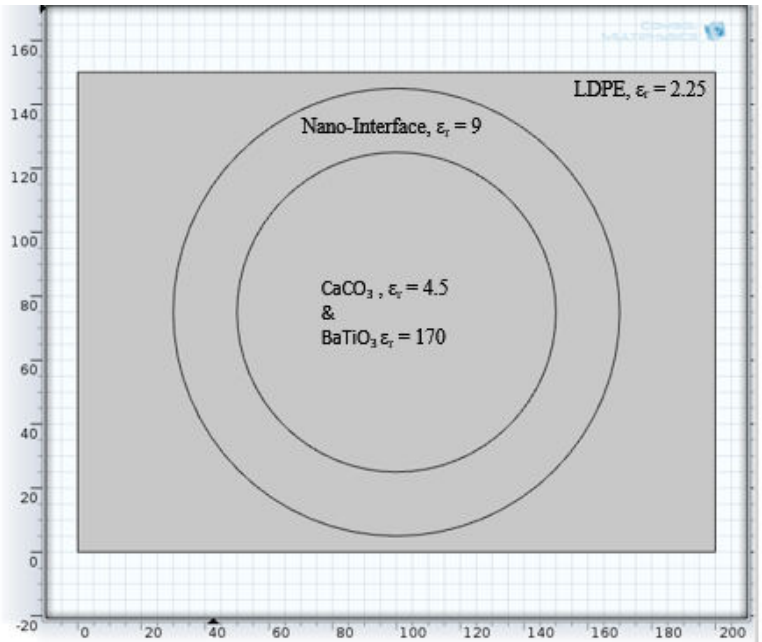

Figure 3.5: Material assigned to changing nano filler material model

3.2.5 Case V: By Changing Interface

In this case, the nano interface relative permittivity has been changed, first the simulation has been run at dielectric constant of 1.5 then for 3.9 as shown in figure 3.6. The change in value will indicator which side of its permittivity works for better insulation.

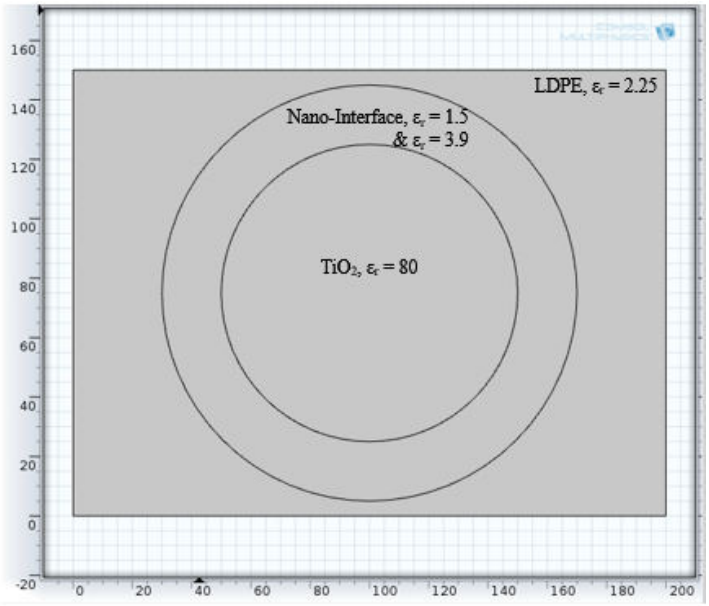

Figure 3.6: Material assigned to changing nano interface material model

3.2.6 Case VI: Effect of Decreasing Interspace Distance

In order to simulate the effect of increasing number of particles in the base material, the distance between them are modelled in decreasing way. First the simulation has been performed when both particles are at a distance of 100 nm as shown in figure 3.7, then for 10 nm as shown in figure 3.8. As the saying goes like "higher side of doping deteriorate the insulation strength". To see the simulation validation of it the case has been chosen to investigate.

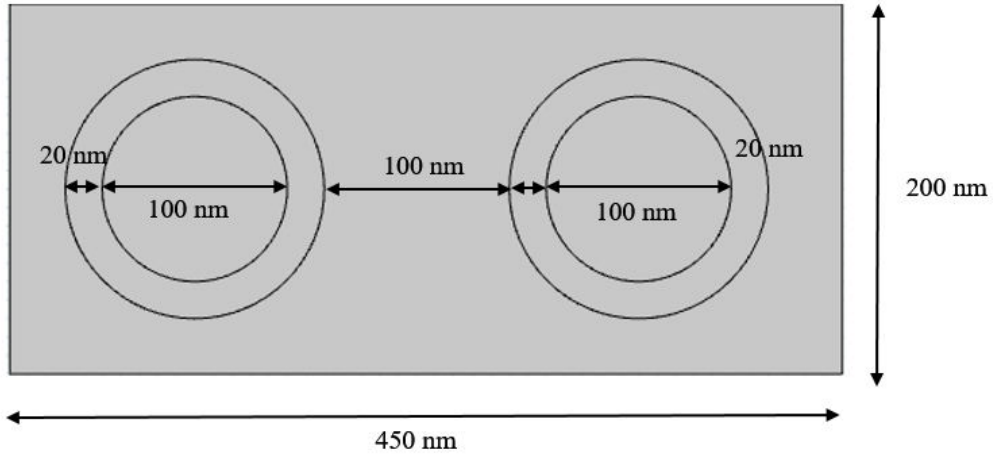

Figure 3.7: Geometric setup of two nanoparticles when 100 nm apart

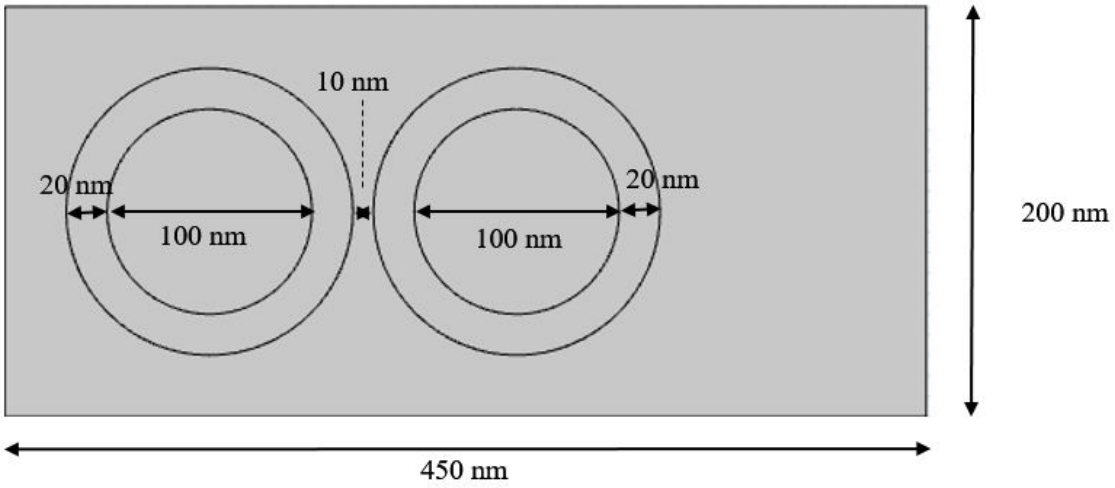

Figure 3.8: Geometric setup of two nanoparticles when 10 nm apart

3.2.7 Case VII: Nano Filler Concentric Model.

- Type –A Configuration: by choosing the inner nanomaterial in increasing order of their relative permittivity and decreasing the outer nanofiller material. As it is clearly seen from the figure 3.9 that outer layer has been increased from permittivity value of 3.9 to 4.5 by changing the filler material from SiO_2 to $CaCO_3$, where the inner filler has been decreased from permittivity value of 2000 to 9 by changing the particle from $SrTiO_3$ to Al_2O_2. Simulation has been performed for both scenarios.

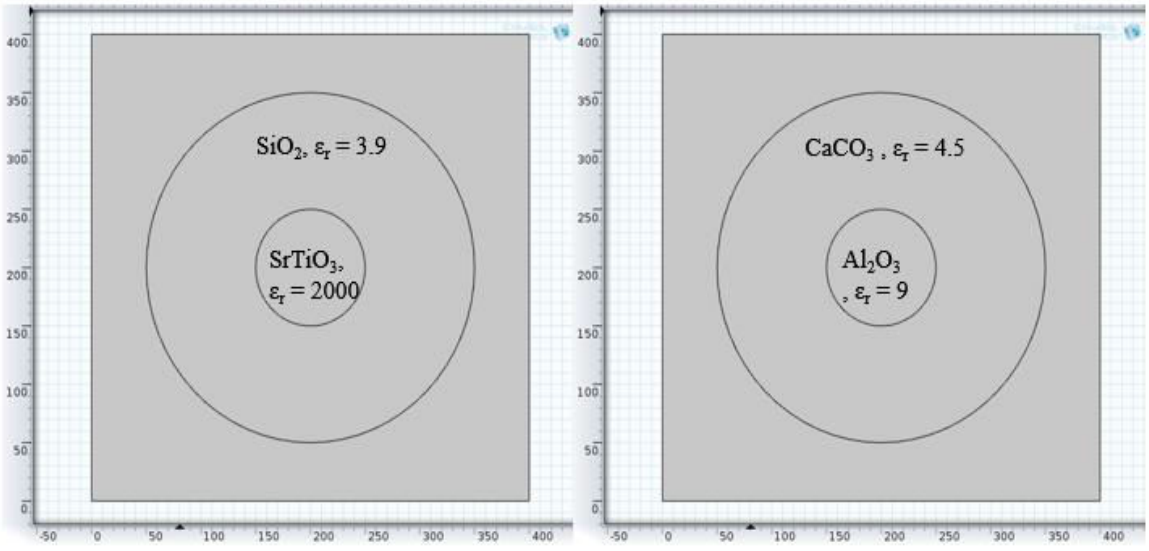

Figure 3.9: Material assigned to Type-A configuration.

- Type- B Configuration: First by choosing the inner nanomaterial in decreasing order of their relative permittivity and increasing the outer nanofiller material. As it is clearly seen from the figure 3.10 that outer layer has been decreased from permittivity value of 22 to 3.9 by changing the filler material from Ta_2O_5 to $CaCO_3$, where the inner filler has been increased

from permittivity value of 3.9 to80 by changing the particle from SiO_2 to TiO_2.

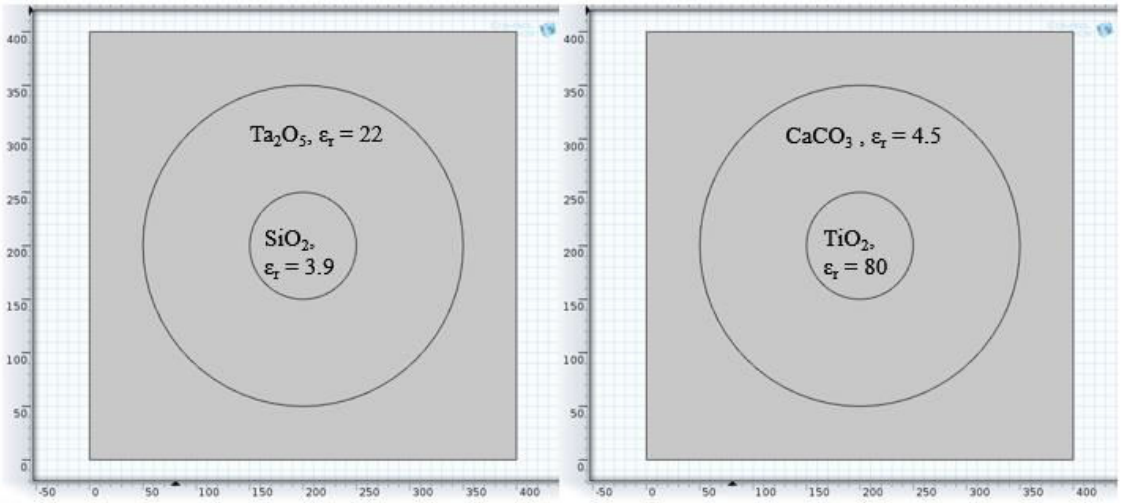

Figure 3.10: Material assigned to Type-B configuration.

- Type-C Configuration: Second case by choosing the inner nano-material in increasing order of their relative permittivity and increasing the outer nanofiller material. As it is clearly seen from the figure 3.11 that outer layer has been increased from permittivity value of 22 to 2000 by changing the filler material from Ta_2O_5 to $SrTiO_3$, where the inner filler has been increased from permittivity value of 9 to80 by changing the particle from Al_2O_3 to TiO_2.

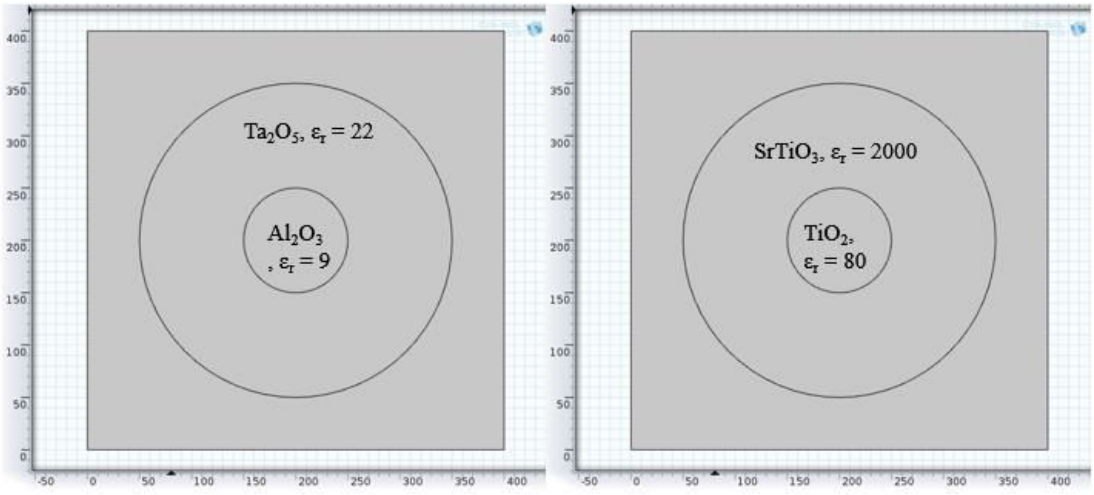

Figure 3.11: Material assigned to Type-C configuration.

- Type-D configuration: Third case by choosing the inner nanomaterial in decreasing order of their relative permittivity and decreasing the outer nanofiller material. As it is clearly seen from the figure 3.12 that outer layer has been decreased from permittivity value of 80 to 9 by changing the filler material from TiO_2 to Al_2O_3, where the inner filler has been decreased from permittivity value of 2000 to 80 by changing the particle from $SrTiO_3$ to TiO_2.

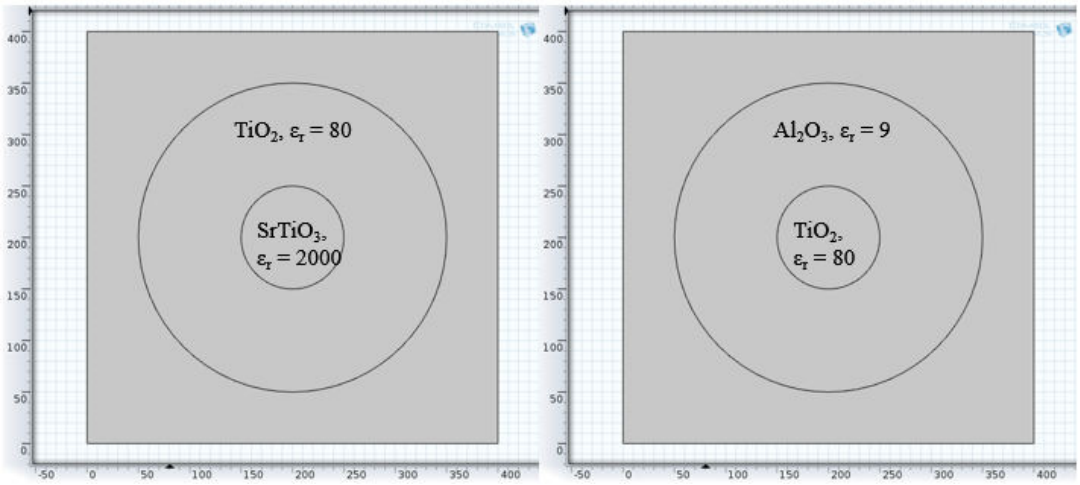

Figure 3.12: Material assigned to Type-D configuration.

3.3 Simulation workflow

This simulation has been again performed on finite element method software COMSOL Multiphysics.

- **Model Environment**

  The model environment is the same as already mentioned in chapter 2.

- **Create Geometry Building**

  As the first step in any FEM problem is to make the geometry, so here in figure 3.13 shows the basic model, which has been used in Case III, IV, V, VI. Figure 3.14 shows the geometry model used in case seventh.

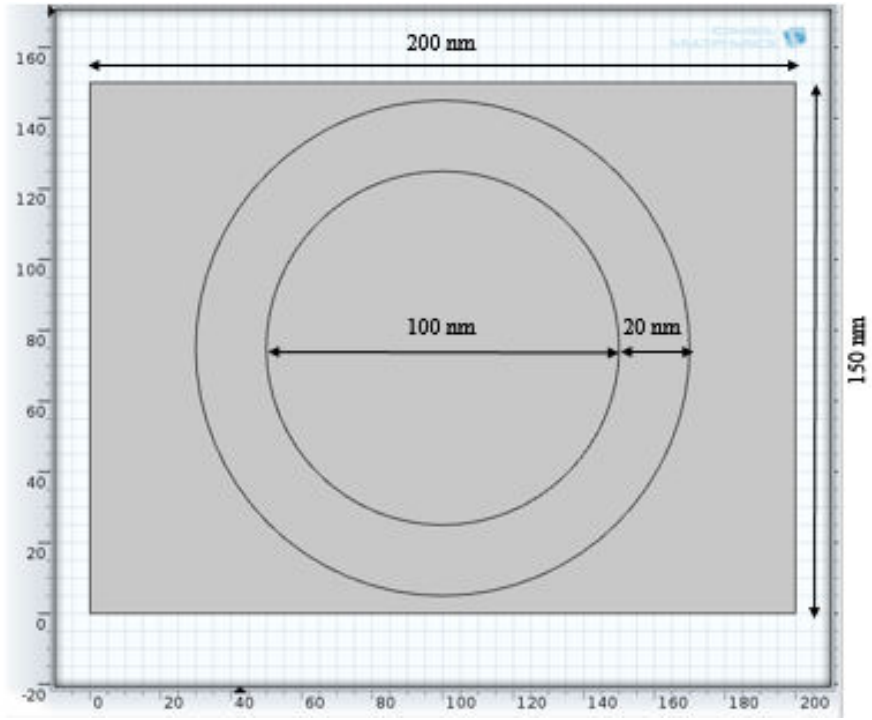

Figure 3.13: Basic geometry model used in case III, IV, V, VI.

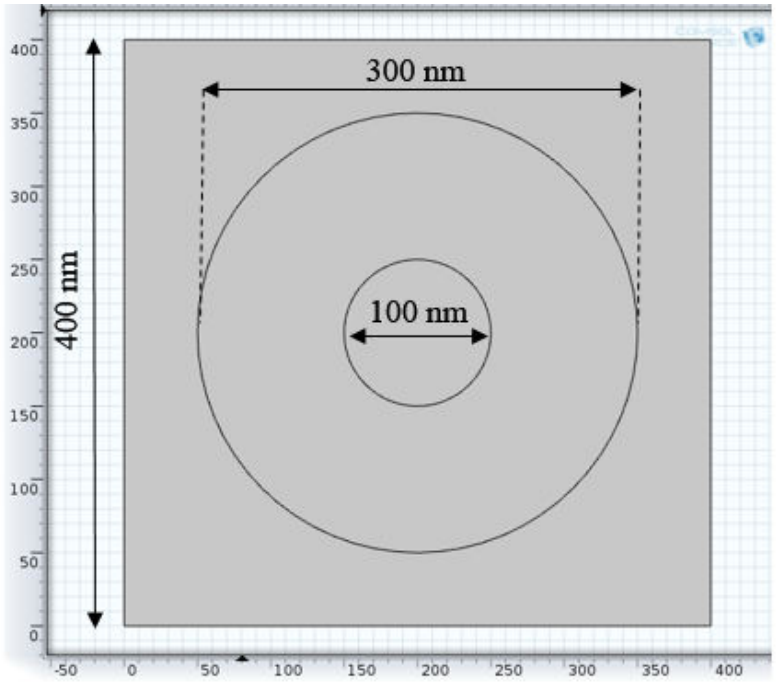

Figure 3.14: Basic geometry model used in case VII.

- **Material Characteristics**

  As this study, consist of nano filler, polymer base, interface area, simulation uses variety of degree of the change in the value of permittivity as a part of its methodology. As study promises the results on the basis of permittivity based response of the material, the large part of material assignation has already discussed in methodology section. The only case six has the purpose to see the effect of action at a distance, so its material properties are fixed as shown in figure 3.15.

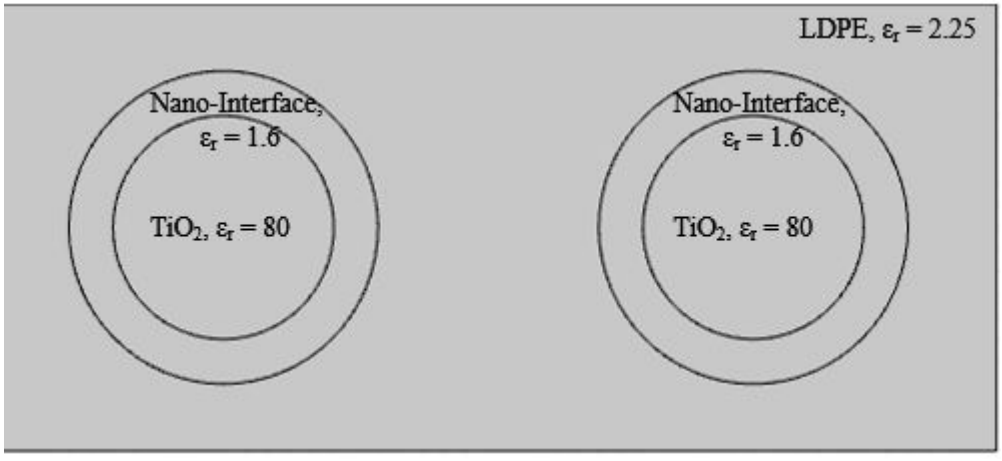

Figure 3.15: Material assigned to case six model

- **Field Equations used.**

  The field equations used here for calculating the electric field from given potential boundary conditions are same Laplace equation as discussed in chapter 2

- **Defining Boundary Conditions**

  Boundary conditions consist of zero charge, charge conservation, ground and potential boundary condition. Charge conservation has been applied to all the domains of all the models of all cases. zero charge is considered to be present on the potential and ground forced fields. Figure 3.16 and 3.17 shows the zero charge boundary conditions of case I and III respectively, but blue lines zero charge boundaries are same for all cases. Now, the potential and ground boundary conditions shown in figure 3.18 and figure 3.19, shows the 33 kV electric potential boundary and ground boundary in case I. Figure 3.20 and 3.21 shows the boundary of electric potential and ground in case III to VII. In every case of investigation, the high and zero potential is in same way. Appling high voltage of 33kV on upper side and 0V to lower side of the nanocomposite material.

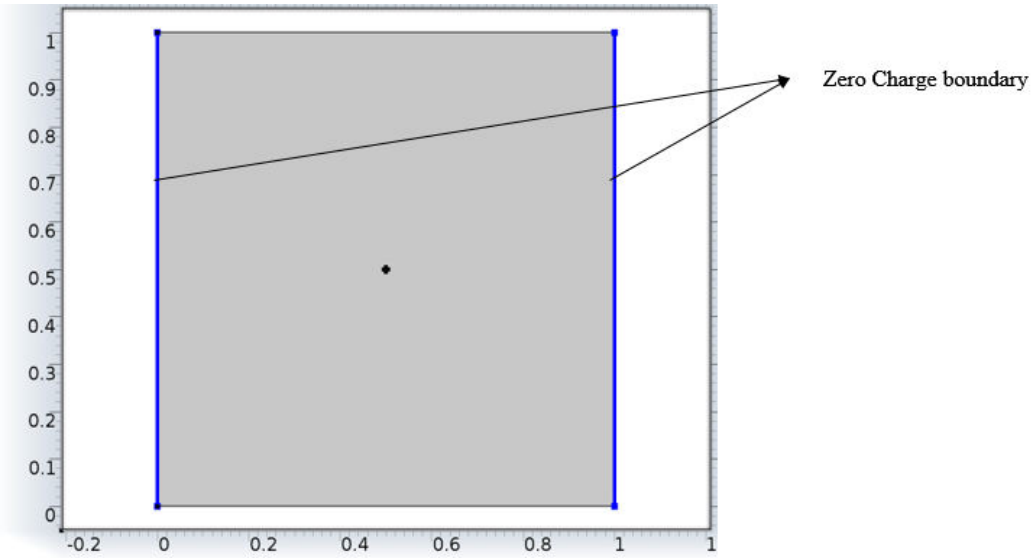

Figure 3.16: Case I zero charge boundaries.

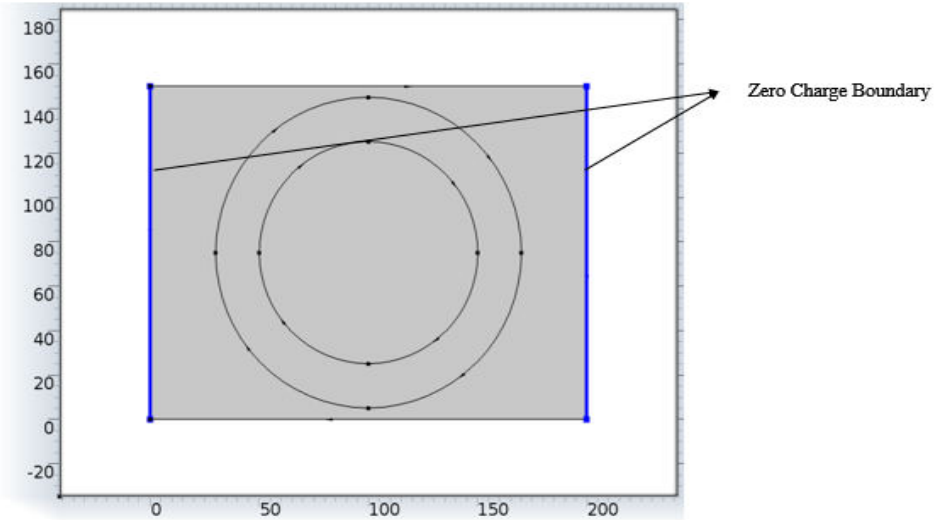

Figure 3.17: Case III zero charge boundaries.

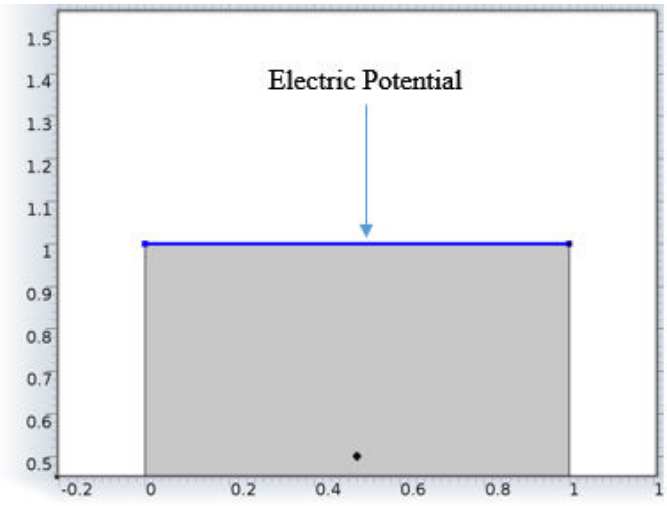

Figure 3.18: Case I potential boundary

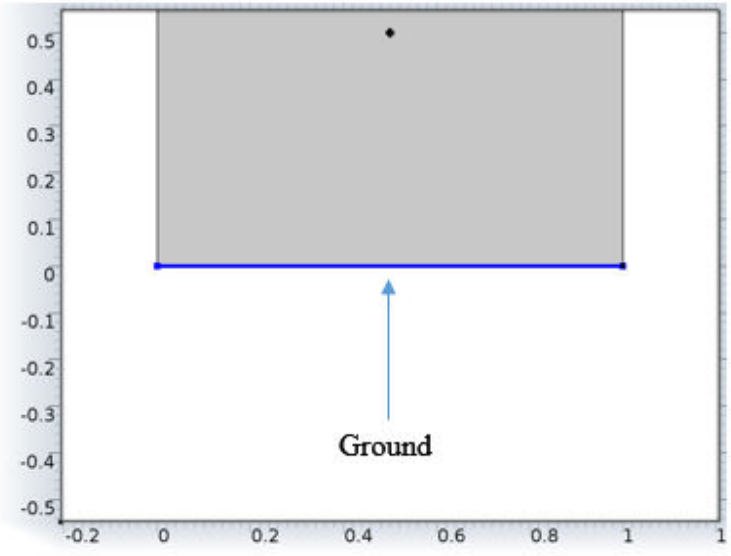

Figure 3.19: Case I ground boundary

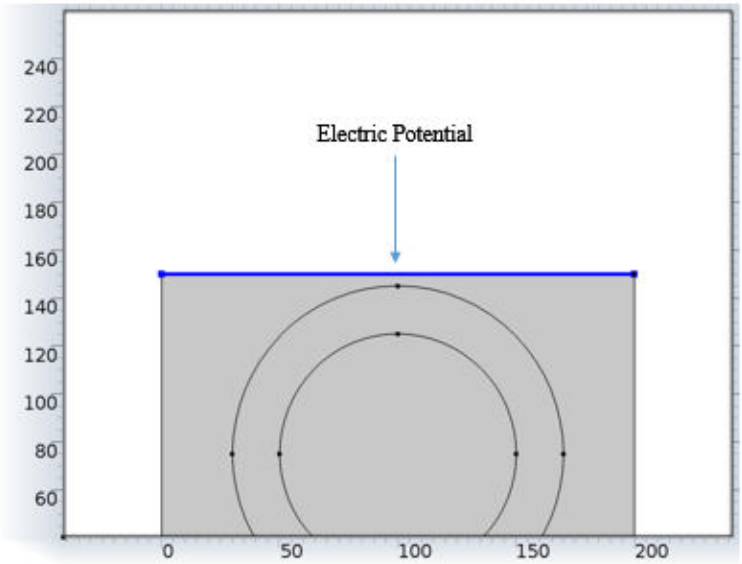

Figure 3.20: Electric potential boundary for case III to VII

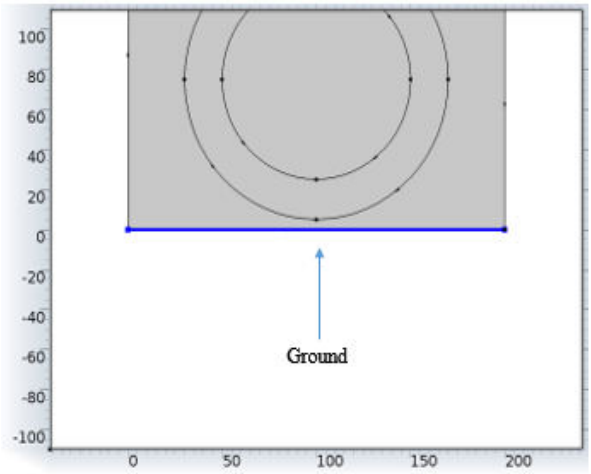

Figure 3.21: Ground boundary for case III to VII

- **Meshing.**

  Physics controlled meshing has been applied in all the cases of investigation, where figure 3.22, figure 3.23 and figure 3.24 shows the meshing of case third, sixth and seventh respectively. Extreme fine mesh has been applied.

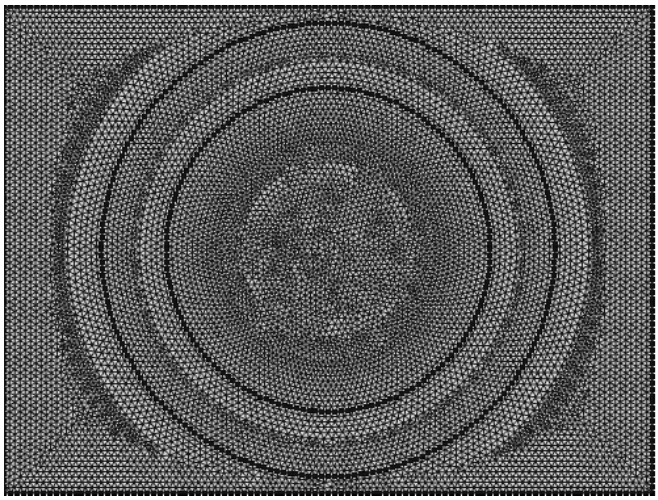

Figure 3.22: Extreme fine meshing of case III

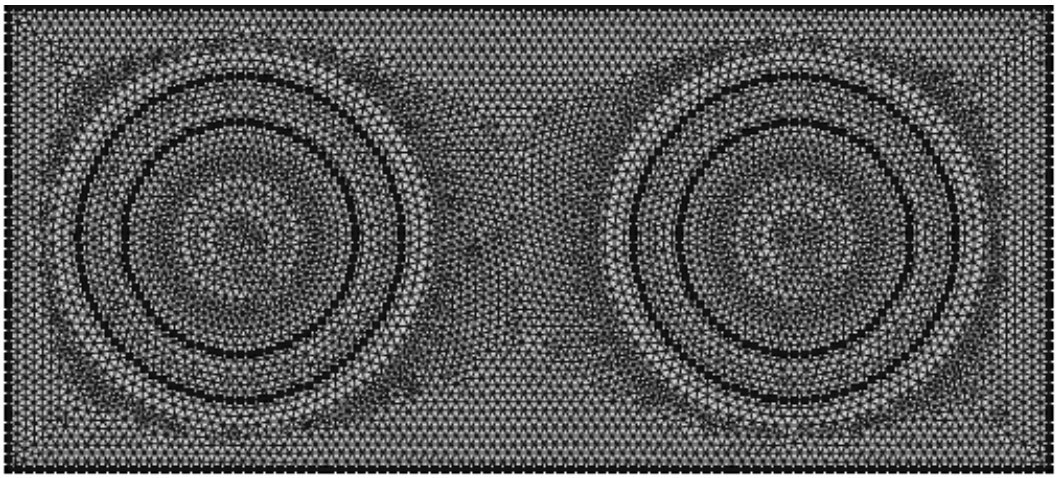

Figure 3.23: Extreme fine meshing of case VI

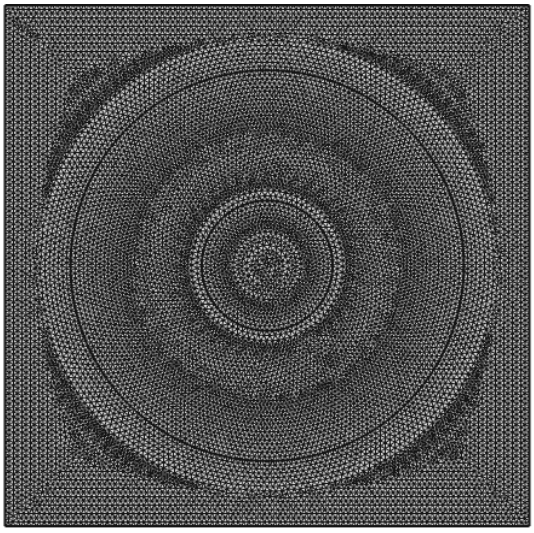

Figure 3.24: Extreme fine meshing of case VII

3.4 Results and Discussion

In case of changing sample permittivity with spherical water void model, as the permittivity of the sample has been increased the E-norm at the void has been decreased, which will prevent the discharge. In figure 3.25 E-norm at permittivity of 10 is 1.0542×10^7 V/m, where it is 8.6527×10^6 V/m as shown in figure 3.26. Significant amount of decrement in the stress of E-norm near water void.

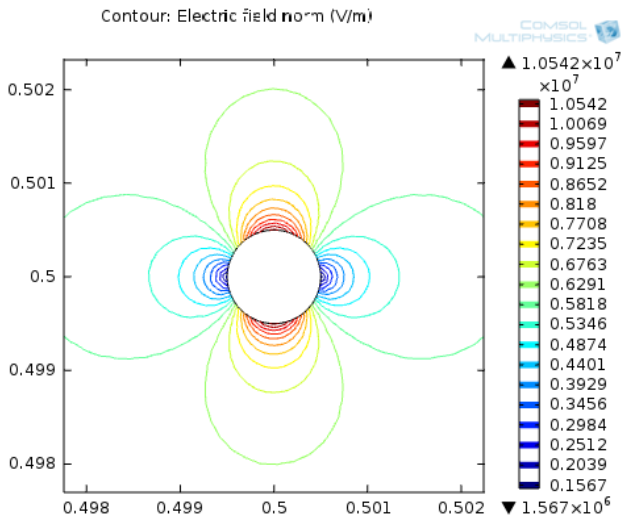

Figure 3.25: E-norm contour at sample permittivity of 10

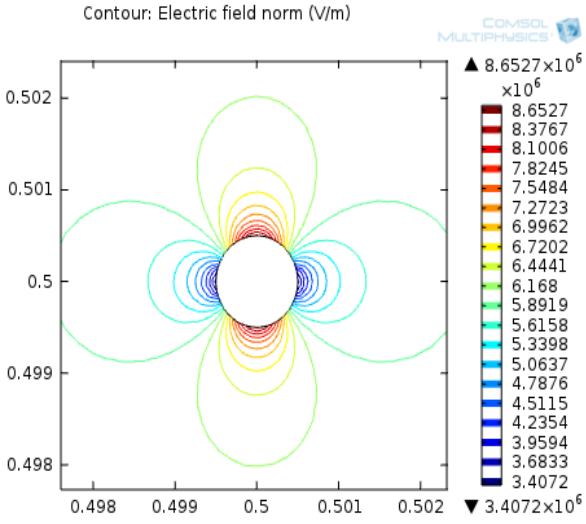

Figure 3.26: E-norm contour at sample permittivity of 30

In case of ellipsoid shape of water void, the value of E-norm is 1.414×10^7 as shown in figure 3.27, where it is 1.0542×10^7 V/m as shown in figure 3.28. Significant amount of increment in the stress of E-norm near ellipsoid water void compared to spherical water void.

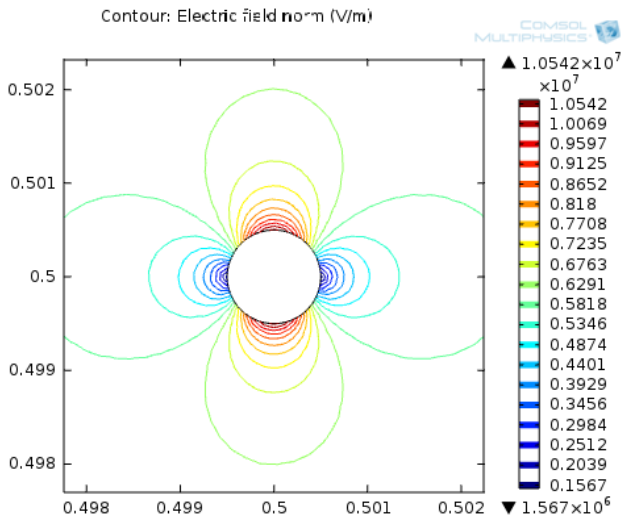

Figure 3.27: E-norm contour of spherical water void

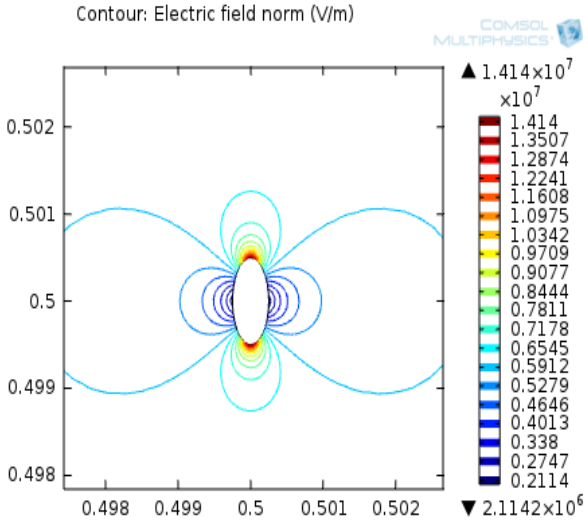

Figure 3.28: E-norm contour of ellipsoid water void

In case of increasing polymer material, the value of E-norm with LDPE base material is 7.704×10^8 as shown in figure 3.29, where it is 8.158×10^8 V/m with epoxy at interface as shown in figure 3.30. Shows the higher permittivity base material is better for insulation as provide high E-norm at interface.

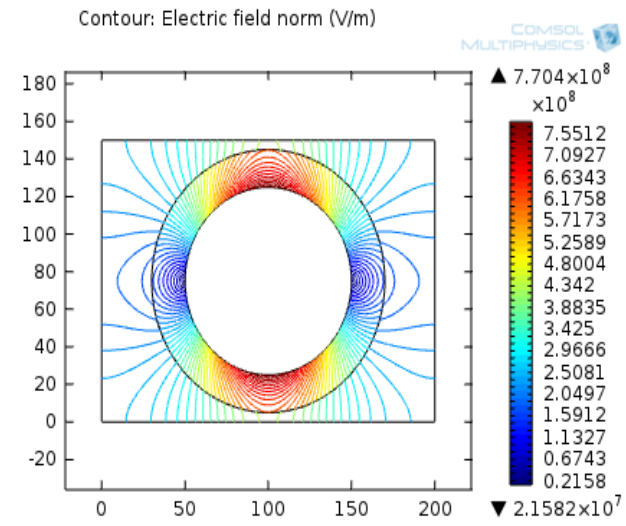

Figure 3.29: E-norm contour during LDPE base material

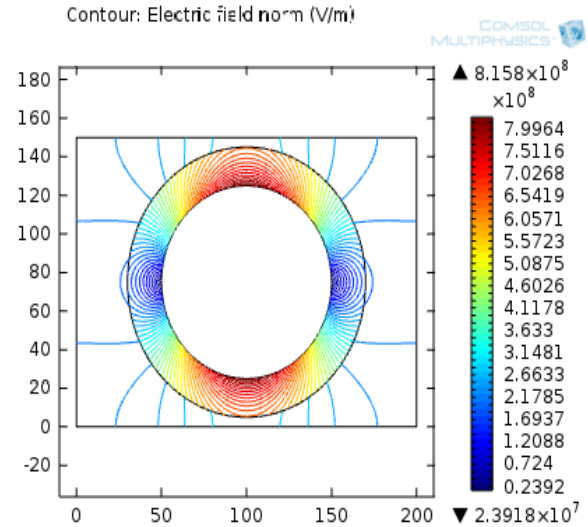

Figure 3.30: E-norm contour during epoxy base material

In case of increasing the filler particle, the value of E-norm at interface with $CaCO_3$ is 2.4981×10^8 as shown in figure 3.31, where it is 6.810×10^9 V/m with $BaTiO_3$ as shown in figure 3.32. It shows that, as the permittivity has been increased from 4.5 to 170 the field strength increased which means filler of higher permittivity value is better to enhance insulation strength.

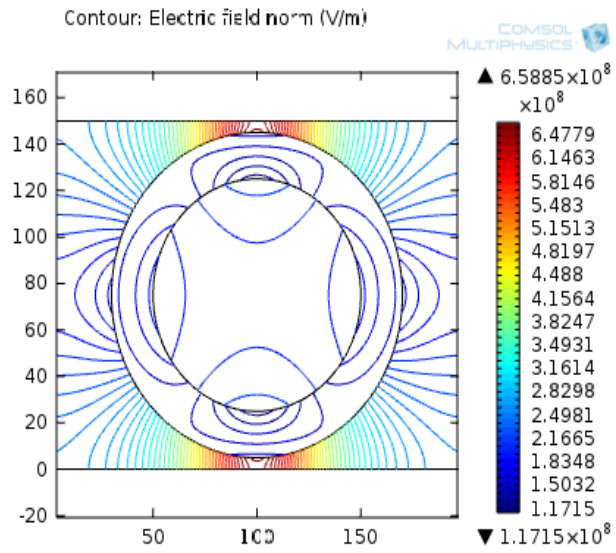

Figure 3.31: E-norm contour for $CaCO_3$ filler material

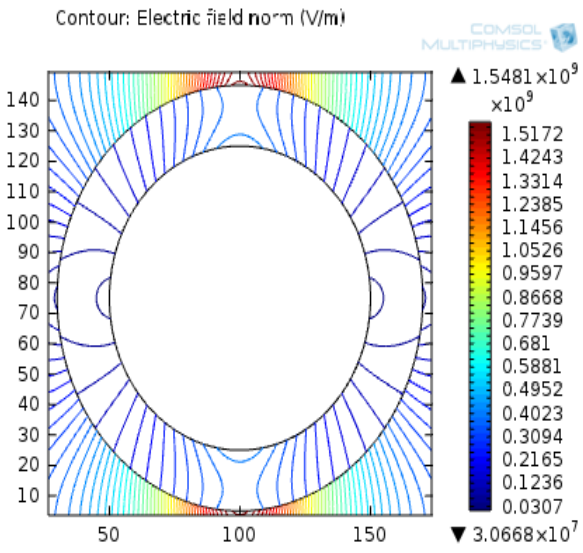

Figure 3.32: E-norm contour for $BaTiO_3$ filler material

In case of increasing interface permittivity, the value of E-norm at interface is 7.6878×10^8 as shown in figure 3.33, where it is 5.6555×10^8 V/m at interface as shown in figure 3.34. It shows that, as the permittivity at interface has been increased from 1.5 to 3.5 the field strength decreased, which means interface of lower permittivity value is better to enhance insulation strength.

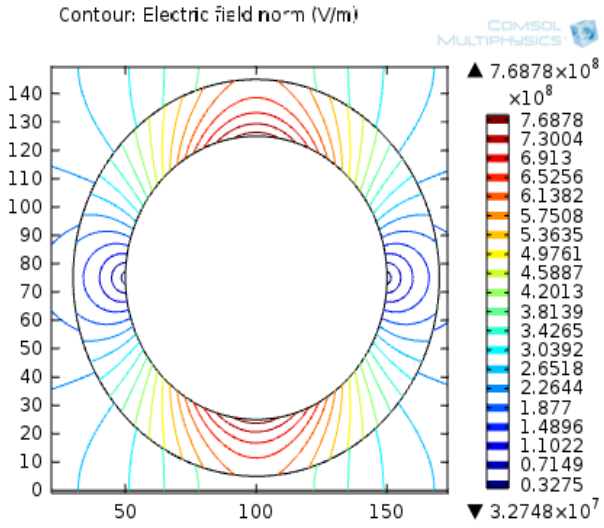

Figure 3.33: E-norm contour at interface permittivity value of 1.5

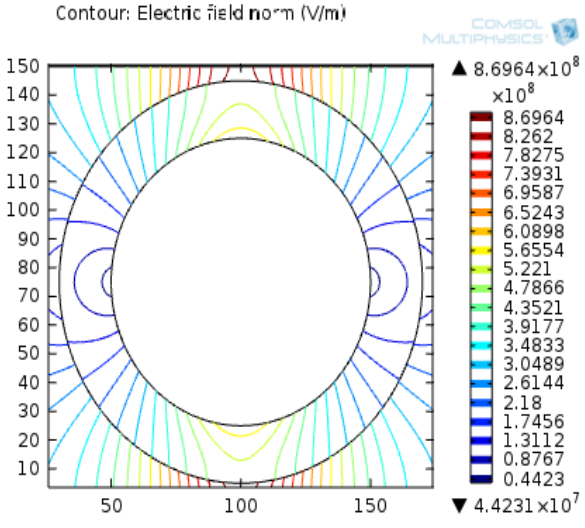

Figure 3.34: E-norm contour at interface permittivity value of 3.5

In case of effect of decreasing interspace distance, the value of E-norm when fillers are 100 nm apart is 6.5525×10^8 as shown in figure 3.35, where it is 6.5349×10^8 V/m at interface when 10 nm apart as shown in figure 3.36. It shows that, as distance decreased from 100 to 10 nm the field strength decreased, means higher filler concentration reduces insulation strength.

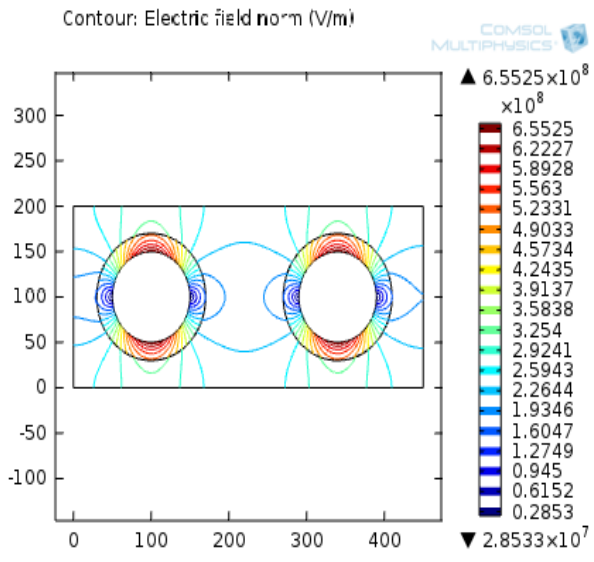

Figure 3.35: E-norm contour when 100 nm apart

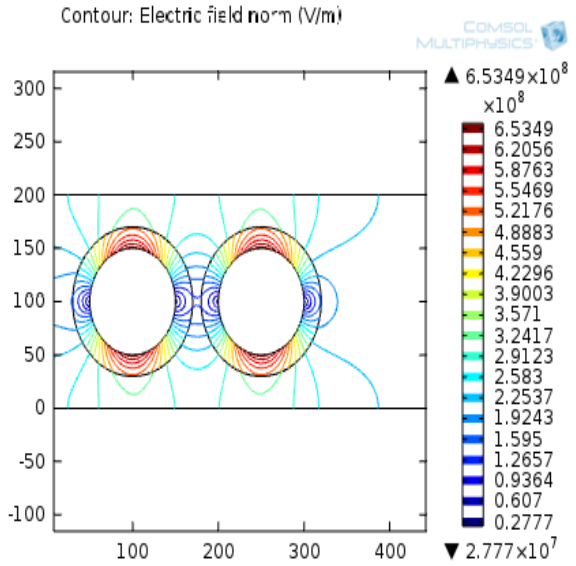

Figure 3.36: E-norm contour when 10 nm apart

In case of concentric nano filler model with Type – A configuration, the E-norm at polymer has been increased from 4.3288×10^9 V/m as shown in figure 3.37 to 4.3452×10^9 V/m as seen from figure 3.38. It shows that as outer permittivity increases and inner filler permittivity decreases the E-norm increases, provide better insulation.

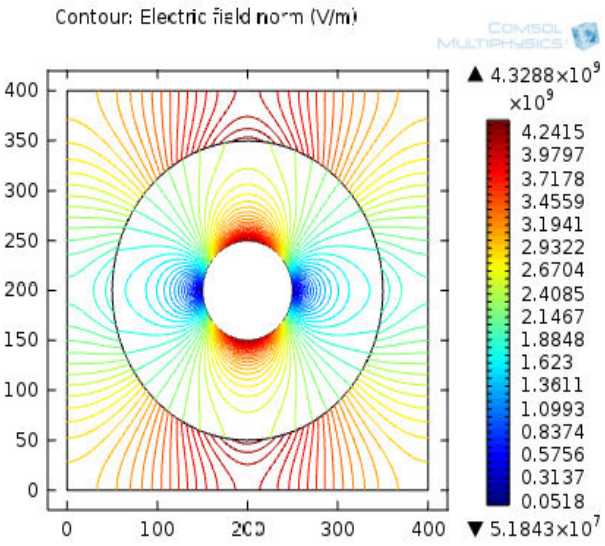

Figure 3.37: E-norm contour when outer permittivity at 3.9 and inner at 2000

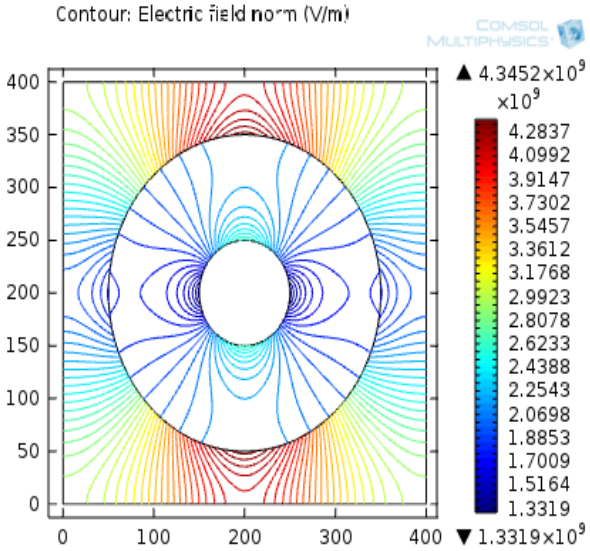

Figure 3.38: E-norm contour when outer permittivity at 4.5 and inner at 9

In case of concentric nano filler model in the Type – B configuration, the E-norm at polymer has been decreased from 8.0027×10^9 V/m as shown in figure 3.39 to 4.6646×10^9 V/m as seen from figure 3.40. It shows that as outer filler permittivity decreases and inner filler permittivity increases the E-norm decreases, provide weak insulation strength.

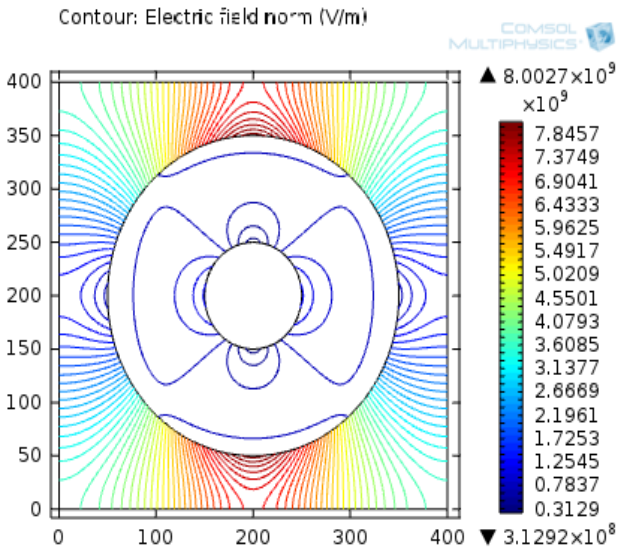

Figure 3.39: E-norm contour when outer permittivity at 22 and inner at 3.9

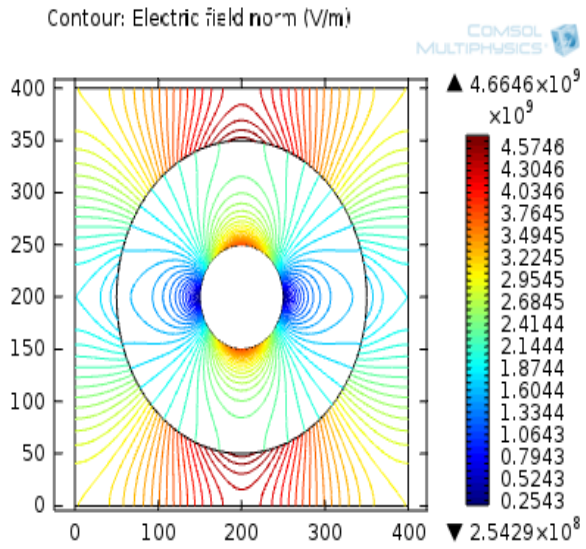

Figure 3.40: E-norm contour when outer permittivity at 4.5 and inner at 80

In case of concentric nano filler model in the Type – C configuration, the E-norm at polymer has been increased from 8.0158×10^{9} V/m as shown in figure 3.41 to 1.0763×10^{10} V/m as seen from figure 3.42. It shows that as outer and inner filler permittivity increases the E-norm increases, again provide better insulation strength.

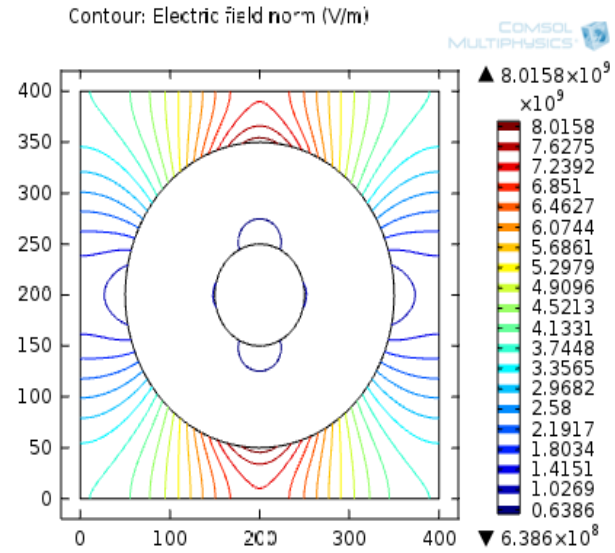

Figure 3.41: E-norm contour when outer permittivity at 22 and inner at 9

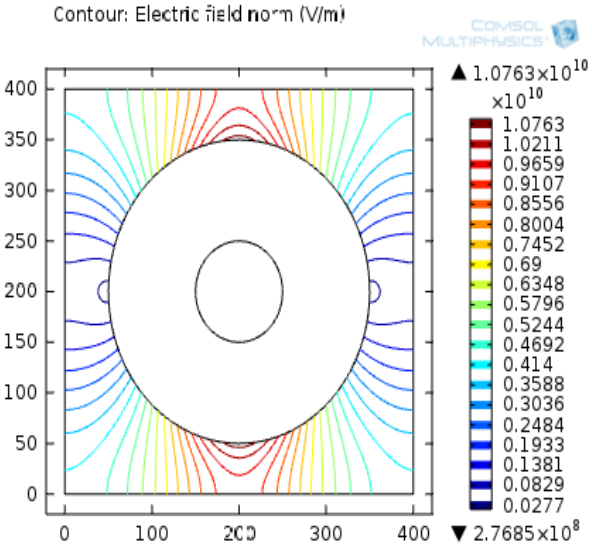

Figure 3.42: E-norm contour when outer permittivity at 2000 and inner at 80

In case of concentric nano filler model in the Type – D configuration, the E-norm at polymer has been increased from 1.0084×10^{10} V/m as shown in figure 3.43 to 6.4579×10^{9} V/m as seen from figure 3.44. It shows that as outer and inner filler permittivity decreases the E-norm decreases, which provide weak insulation strength.

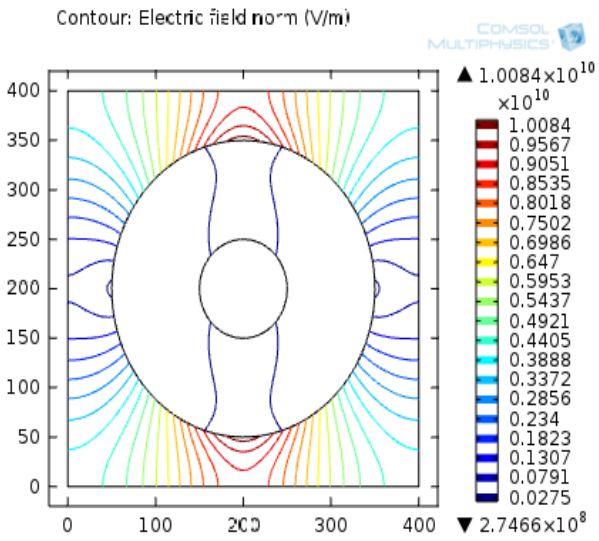

Figure 3.43: E-norm contour when outer permittivity at 80 and inner at 2000

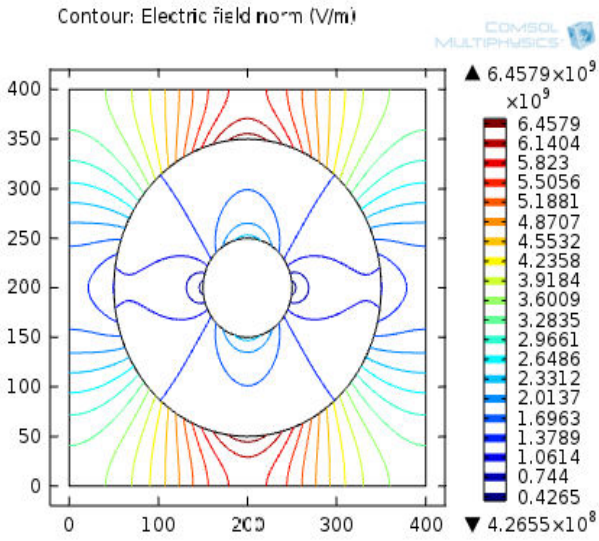

Figure 3.44: E-norm contour when outer permittivity at 9 and inner at 80

CHAPTER 4
CONCLUSION AND FUTURE SCOPE

4.1 Conclusion

In this dissertation, systematic investigation has been carried out on dielectrics from overhead transmission lines to underground cable insulation. Polymer overhead insulator investigation focuses on environmental factor which deteriorations it. Nanocomposite underground insulation focuses on the way to understand the nature of the nanodielectrics for better insulation strength.

4.1.1 Overhead Insulators

In this case, visual observations showed that the intensity of the local electric field at the triple point junction is high in both cases. In first case of investigation simulation results show that E-norm in humid air is 23.4% higher or 1.3 times higher in comparison to dry air. The results also showed that the field enhancement ratio in humid is 2 times, wherein the dry air it is 1.5 times. In case of normalized polarization density distribution, visual observations showed that the polarization density at the triple point junction is highest and maximum polarization is shifted to its ends in both of the cases. Simulation results show that P-norm in humid air is 9.42% higher or 1.10 times higher in comparison to dry air. In second case of investigation, the E-norm and P- norm has increased by 10.45 % and 5.85 % respectively as volume has increased. In addition, results also showed that increasing volume means triple point junction more close to the voltage terminal hence the electrostatic parameters has also been increasing with the increasing volume. The visual observation in the normalized electric field showed that the intensity of the local electric field at the triple point junction is high as the value of contact angle and dust relative permittivity increases. Simulation results also show that E-norm incremental percentage and P-norm incremental percentage increases as the contact angle and dust relative permittivity increases. E-norm enhancement ratio and P-norm intensification percentage increases significantly as the value of contact angle and dust relative permittivity increases. Additionally, from the study it has inferred that the wader drop under the influence of urea is more susceptible to the electrostatic effects at the triple point junction of the drop.

A systematic investigation of the electrostatic effects on the triple point junction due to the presence of the deposited particle near water drops during initial stages under high voltage stress. In this dissertation, four cases have been investigated from the electric field and

polarization density distribution point of view. First by changing particle position, second by changing relative permittivity of the particle, third by changing the number of particles and forth by changing the particle size. The simulation results showed that the electric field and polarization density has been increased as particle came near to water drop, as relative permittivity of the particle is increased, as the number of particles has increased and as the size of the particle has decreased. Though the increment in the electric field and polarization density in case of increasing the number of particles and relative permittivity is not significant but it has shown the increasing nature on triple point junction. The electric field and polarization density in presence of a particle on TPJ have been increased significantly in comparison to the absence of it.

The visual observation from all four cases of the investigation showed that the unevenness in the electric field due to the presence of particle or micrometre settled bumped has increased the electric field on TPJ of a water drop. Visual observations also showed that at the triple point junction, the electric field and polarization density has been shifted from both sides ends of the drop to the left side end where the particle heterogeneity is present.

Hence, this work concludes that the water drop under humid air conditions, large volume, higher contact angle, higher pollution layer permittivity and the presence of micrometre particle or micrometre settled bumped on the surface is highly susceptible to all kinds of electrostatic phenomenon, dominating at the edge, this establishes a relation between the electrical field and environment conditions.

Finally, the practical importance of this work is that it can be used to effectively learn about the initial behaviour of the water drop on clean SIR insulator surface using the finite element method.

4.1.2 Nano-dielectrics

It has been seen that, as the permittivity of the nanocomposite increases the chances of discharge from spherical water voids gets decreases, but in comparison to ellipsoid water void the chances due to ellipsoid void to cause partial discharge is still high. Secondly, it has been concluded that higher the permittivity of the base material and nano filler enhances the nano dielectric strength. Nano interface is considered as the cause for better insulation strength, but as its understanding is largely unknown. The simulation results showed that lower the value of the permittivity at interface better the strength of dielectric, as lower side interface enhancing the electric filed strength at the interface. So, from this we can conclude that any nanocomposite giving better insulation must have a lower permittivity at interface.

A case has been verified where, as the interparticle distance decreases the electric field at interface decreased which weak the dielectric strength. This case infer that the large number of doping may lead to bad insulator strength.

At last, a new approach has been investigated which results in finding the best configuration for better insulation. Simulation results showed that if inner nanomaterial in increasing order of their relative permittivity and decreasing the outer nanofiller material or both inner and outer nanomaterial in increasing order of their relative permittivity can provide better insulation.

Finally, the practical importance of this work is that it can be used to understand nano interface in nanodielectrics and future investigators can use it as a guide to choose material for their next experiment in order to obtain better insulation. Keeping the note that all these investigations results are based on permittivity values only, so the true results may vary. However, within its domain this work provides insight on nano interface behaviour.

4.2 Future Scope

- ✓ *Following factors are still needed to be investigated on the water drop model.*
  - By considering the charge flow in electric current physics model in COMSOL Multiphysics.
  - By varying the conductivity of pollution factors.
  - By taking pair and multiple drop model.
  - By incorporation the deformation pattern of the drop.
  - After all, by moving towards the real word 3D insulator model, hence analysis of environmental exposure effect on the actual 3D model in FEMLAB.
- ✓ *Nanocomposite materials require further investigation, as mentioned below*
  - By simulating actual water tree channel.
  - By varying the size of the nano particle.
  - Comparison analysis of circular vs rectangular nano filler and interface.
  - By incorporation of water void/ air void inside interface area of the nanocomposite.
  - Nano filler concentric configuration needs to studied again by considering the interface area also.

LIST OF PUBLICATIONS

[1] **V. Srivastava, B. S. Rajpurohit, M. Kaur**, "Investigation of Water Drop on SIR Insulator for High Voltage Transmission Line Using FEM," *8th IEEE Power India International Conference (PIICON-2018)*, Kurukshetra, Haryana, India; December 10-12, 2018.

[2] **V. Srivastava, B. S. Rajpurohit**, **M. Kaur**, "Numerical Analysis of Water drop on SIR Insulator for High Voltage Power Transmission Line", *8th IEEE Power India International Conference (PIICON-2018)*, Kurukshetra, Haryana, India; December 10-12, 2018.

[3] **V. Srivastava, B. S. Rajpurohit, M. Kaur,** "Numerical Investigation of Particle Effect on Water Drop under High Voltages SIR Insulator", *3rd International Conference on High Voltage Engineering and Technology (ICHVET 2019)*, CPRI UHVRL Hyderabad, Telangana, India; Feb 07-08, 2019

REFERENCES

[1] J. Looms, Insulators for High Voltages. ser. Energy Engineering Series. Peregrinus,1988.

[2] S. R. B., “A novel technique for enhancing the pollution flashover strength of ceramic disc insulators," Ph.D. dissertation, Department of Electrical Engineering, IISc, Bangalore, India, 2010.

[3] Hanley, T. L.; Burford, R. P.; Fleming, R. J.; Barber, K. W. IEEE Electrical Insulation Magazine 2003, 19, (1), 13-24.

[4] Khalil, M. S. IEEE Electrical Insulation Magazine 1997, 13, (6), 35-47.

[5] Shen, Y. DC Cable Systems with Extruded Dielectrics; 2004.

[6] F. Aouabed, A. Bayadi, A. E. Rahmani and R. Boudissa, "Finite element modelling of electric field and voltage distribution on a silicone insulating surface covered with water droplets," IEEE Transactions on Dielectrics and Electrical Insulation, vol. 25, no. 2, pp. 413-420, April 2018

[7] Reynders, J.P. & Jandrell, I.R. & Reynders, S.M. “Review of aging and recovery of SIR insulation for outdoor us, ” IEEE Transactions on Dielectrics and Electrical Insulation, vol 6, pp. 620 – 631, 1999.

[8] N. Yoshimura, S. Kumagai, S. Nishimura, "Electrical and environmental ageing of SIR used in outdoor insulation", IEEE Transactions on Dielectrics and Electrical Insulation, vol. 6, pp. 632-650, 1999.

[9] C. Zhao, M. Zhu, H. Mei, L. Wang and Z. Guan, "Influence of environmental factors on hydrophobicity transfer property of SIR material," 2015 IEEE Electrical Insulation Conference (EIC), Seattle, WA, pp. 596-599, 2015.

[10] R. Hackam, "Outdoor high voltage polymeric insulators," Proceedings of 1998 International Symposium on Electrical Insulating Materials, 1998 Asian International Conference on Dielectrics and Electrical Insulation, 30th Symposium on Electrical Insulating Ma, Toyohashi, pp. 1-16, Japan, 1998.

[11] E.A. Cherney, R.S. Gorur et.al, "Round robin testing of RTV SIR coatings for outdoor insulation," IEEE Transactions on Power Delivery, vol. 11, no. 4, pp. 1881-1887, October 1996.

[12] Zhicheng Guan, Liming Wang, Bo Yang, Xidong Liang and Zhi Li, "Electric field analysis of water drop corona," IEEE Transactions on Power Delivery, vol. 20, no. 2, pp. 964-969, April 2005.

[13] Mr. G. Satheesh, Dr. B. Basavaraja, Dr. Pradeep M. Nirgude, “Electric Field along Surface of SIR Insulator under Various Contamination Conditions Using FEM”, in International Journal of Scientific & Engineering Research, Volume 3, Issue 5, May-2012.

[14] S. Feier-Iova and V. Hinrichsen, "Partial discharge inception voltage of water drops on insulating surfaces stressed by electrical field”, IEEE Electrical Insulation Conference, Montreal, QC, pp. 21-25, 2009.

[15] Wang, X and Kumagai, S and Yoshimura, N. , “Relation between Hydrophobicity and Surface Roughness of SIR Insulator before and after Aging in Acid Rain” , IEEJ Transactions on Fundamentals and Materials, 1999.

[16] Wang, Song and Yuan, Tian and Zhou, Jun and Wang, Qian-yu,” Surface Roughness Effect on the Hydrophobicity Characteristic of Operating Composite Insulators” in 3rd International Conference on Electric and Electronics, Atlantis Press, 1951-6851, 2013.

[17] Selection and dimensioning of high-voltage insulators intended for use in polluted conditions - Part 1: Definitions, information and general principles, IEC TS 60815-1:2008, 2008.

[18] G. Moustafa and R. A. Abd El-Aal, "Break down voltage of air gaps as influenced by dust storm," 2016 Eighteenth International Middle East Power Systems Conference, Cairo, pp. 567-572, 2016.

[19] Andritsch, T.M., “Epoxy Based Nano dielectrics for High Voltage DC Applications: Synthesis, Dielectric Properties and Space Charge Dynamics”, Electrical Sustainable Energy, 2010-11-02.

[20] S. Zhong, Z. Dang, W. Zhou and H. Cai, "Past and future on nanodielectrics," in IET Nanodielectrics, vol. 1, no. 1, pp. 41-47, 4 2018.

[21] T. Arakane, T. Motchizuki, N. Adachi et al., "Space charge accumulation properties in XLPE with carbon nano-filler", IEEE International Conference on Condition Monitoring and Diagnosis, pp. 328-331, September 2012.

[22] Z.M. Dang, J.K Yuan, J.W. Zha et al., "Fundamental processes and applications of high-permittivity polymer-matrix composites", Prog. Mater Sci., vol. 57, pp. 660-723, 2012.

[23] Q. Chen, Y. Shen, S.H. Zhang et al., "Polymer-based dielectrics with high energy storage density", Annu. Rev. Mater. Res., vol. 45, pp. 433-458, 2015.

[24] W.A. Izzati, Y.Z. Arief, Z. Adzis et al., "Partial discharge characteristics of polymer nanocomposite materials in electrical insulation: a review of sample preparation techniques analysis methods potential applications and future trends", Science World Journal, vol. 2014, pp. 1-14, 2014.

[25] T.J. Lewis, "Nanometric dielectrics", IEEE Transactions on Dielectrics and Electrical Insulation, vol. 1, no. 5, pp. 812-824, 1994.

[26] T. Tanaka, M. Kozako, N. Fuse et al., "Proposal of a multi-core model for polymer nanocomposite dielectrics", IEEE Transactions on Dielectrics and Electrical Insulation, vol. 12, no. 4, pp. 669-681, 2005.

[27] Barber, P.; Balasubramanian, S.; Anguchamy, Y.; Gong, S.; Wibowo, A.; Gao, H.; Ploehn, H.J.; Zur Loye, H.-C. Polymer Composite and Nanocomposite Dielectric Materials for Pulse Power Energy Storage, pp. 1697-1733, February 2009.

[28] Peng Simin, Zeng, Qibin Yang, XiaoHu,JunQiu,Xiaohui He,Jinliang, "Local Dielectric Property Detection of the Interface between Nanoparticle and Polymer in Nanocomposite Dielectrics", Scientific Reports, Nature Research journals, Articles, Vol.6, 2016/12/13.

[29] D. Kavitha, T. K. Sindhu and T. N. P. Nambiar, "Impact of permittivity and concentration of filler nanoparticles on dielectric properties of polymer nanocomposites," in IET Science, Measurement & Technology, vol. 11, no. 2, pp. 179-185, March 2017.

[30] Wang, Wenxuan, Yang, Ying, "The Synergistic Effects of the Micro and Nano Particles in Micro-nano Composites on Enhancing the Resistance to Electrical Tree Degradation" Scientific Reports, Nature Research journals, 17/05/2017.

[31] Xin Zhang, Weiwei Chen, Jianjun Wang, Yang Shen, Lin Gu , Yuanhua Lin and Ce-Wen Nan, “Hierarchical interfaces induce high dielectric permittivity in nanocomposites containing TiO_2@$BaTiO_3$ nanofibers”, The Royal Society of Chemistry, Nanoscale, 2014**.**

[32] R. G. Olsen, T. Zhao and M. G. Comber, "Discussion of Calculation of electric field and potential distribution along nonceramic insulators considering the effects of conductors and transmission towers" , IEEE Transactions on Power Delivery, vol. 15, no. 4, pp. 1353-1354, October 2000.

[33] E. Asenjo S., N. Morales O. and A. Valdenegro E., "Solution of low frequency complex fields in polluted insulators by means of the finite element method," IEEE Transactions on Dielectrics and Electrical Insulation, vol. 4, no. 1, pp. 10-16, February 1997.

[34] Hossein Daneshpajooh, “What is the difference between ANSYS and COMSOL?” Internet: https://www.quora.com/What-is-the-difference-between-ANSYS-and-COMSOL, Mar 8, 2016 [July. 29, 2018].

[35] M.Y.Kamel & , M.AbouelSaad & El-Wakeel, Amged & A Hassan, “Influences of Water Droplet Size and Pollution Layer Permittivity On The Electric Field And Potential Distribution On A Polluted Insulator Surface”, 2008.

[36] C. Song, Q. Chen, X. Wang, L. Wen and T. Zheng, "Deformation and motion behaviour of droplets in a non-uniform electric field," 2015 IEEE 11th International Conference on the Properties and Applications of Dielectric Materials (ICPADM), Sydney, NSW, Australia, pp. 652-655, July 2015.

MTech Thesis

ORIGINALITY REPORT

10%	8%	7%	0%
SIMILARITY INDEX	INTERNET SOURCES	PUBLICATIONS	STUDENT PAPERS

PRIMARY SOURCES

1	tuprints.ulb.tu-darmstadt.de Internet Source	<1%
2	digital-library.theiet.org Internet Source	<1%
3	eprints.uthm.edu.my Internet Source	<1%
4	dspace.cc.tut.fi Internet Source	<1%
5	www.mdpi.com Internet Source	<1%
6	publications.lib.chalmers.se Internet Source	<1%
7	Yong Liu, Xianghuan Kong, Yafeng Wu, Boxue Du. "Dynamic Behavior of Droplets and Flashover Characteristics for CFD and Experimental Analysis on SiR Composites", IEEE Access, 2019 Publication	<1%
	dspace.thapar.edu:8080	